[AMERICAN JOURNAL OF SCIENCE, VOL. 276, SUMMER, 1976, P. 883-916]

# COMPARISON OF METHODS FOR CALCULATING AND EXTRAPOLATING EQUILIBRIA IN P–T–$X_{CO_2}$ SPACE

D. M. KERRICK and J. SLAUGHTER*

Department of Geosciences,
The Pennsylvania State University,
University Park, Pennsylvania 16802

ABSTRACT. Accurate equations for the P–T–$X_{CO_2}$ extrapolation of equilibria can be derived from log K-1/T diagrams providing that two narrow, but widely spaced, experimental brackets are available. Calculation of the change in the equilibrium constant with changing pressure should incorporate the corresponding variation in the activity coefficients of the gas species involved in the reaction. The most serious source of error in these equations arises from the lack of precise experimental location of an equilibrium curve, as illustrated by examples in the system CaO–MgO–$SiO_2$–$CO_2$–$H_2O$. Where only one narrow experimental bracket is available, we prefer extrapolation from this bracket using Greenwood's (1967a) "constant enthalpy" expression (for isobaric calculations) or an equation involving $G_{H_2O}$ and $G_{CO_2}$ for isobaric and polybaric P–T–$X_{CO_2}$ extrapolations. With accurate entropy data for solid phases, accurate extrapolations of many equilibria can be accomplished from one narrow (± 5°-10°C) experimental bracket. However, correction for non-ideal fluid mixing is important for extrapolations in the lower temperature range (<500°C). Uncertainties in the tabulated thermodynamic data introduce a negligible error in these extrapolations. However, for equilibria involving aluminous phases, variation in Al/Si disorder can introduce differences in the extrapolated curves, warranting several widespread experimental brackets in such cases. Since derivation of stable equilibria by coupling other stable or metastable equilibria compounds the uncertainties, we advocate the direct experimental determination of the stable equilibria of interest.

## INTRODUCTION

Although there exists considerable experimental data for many mixed-volatile ($H_2O$–$CO_2$) equilibria, relatively few reactions have been accurately determined over a *wide range* of P–T–$X_{CO_2}$ space. Since such direct experimental determination is time consuming, it is clearly advantageous to develop accurate methods for extrapolating equilibria in P–T–$X_{CO_2}$ space from a minimum of reliable experimental data. Accordingly, it is the purpose of this paper to evaluate and intercompare the various methods for such extrapolations. We will discuss three main equations used for these calculations. In so doing, we will illustrate the *basic* equivalence of the various expressions, evaluate sources of uncertainty in each approach, and intercompare the various methods by P–T–$X_{CO_2}$ extrapolations on the same equilibria. Each style of calculation is discussed separately only because many authors have confined their treatment to one particular style of calculation; however, such separation is not meant to imply any fundamental differences between the various equations used, since all these equations can be derived from the same basic expression. Finally, we include a short discussion of some important points concerning experimentation. This paper is an elaboration of the discussions in Kerrick (1974) and in Slaughter, Kerrick, and Wall (1975).

* Present address: E. I. C. Inc., 55 Chapel Street, Newton, Massachusetts 02160

SYMBOLS

$a_i$ = activity of component i
$(\Delta C_p)_r$ = isobaric change in heat capacity for a reaction
$f_i^*$ = fugacity of component i in a gas mixture
$f_i^\circ$ = fugacity of pure component i
$\Delta G^\circ_r$ = standard state free energy change of a reaction
$\Delta G_r$ = free energy change of a reaction
$G_{CO_2}$, $G_{H_2O}$ = free energies of pure $CO_2$ and $H_2O$ at P and T
$\overline{G}_i$ = partial molar free energy of component i
$\Delta H^\circ_r$ = standard state enthalpy change for a reaction
K = equilibrium constant, standard state unspecified
$K_X$ = equilibrium constant expressed in terms of mole fractions of gas components; implies a standard state of all phases at P and T
$K_f$ = equilibrium constant expressed in terms of fugacities of gas components; implies a standard state for solids at P and T and for gases at 1 atm and T
$n_i$ = stoichiometric coefficient of component i in a balanced chemical reaction
P = pressure
R = gas constant
$\Delta S^\circ_r$ = standard state entropy change of a reaction
$\Delta S^\circ_s$ = standard state entropy change for solid phases of a reaction
T = temperature (°K in thermochemical equations)
$\Delta V^\circ_r$ = standard state volume change of a reaction
$\Delta V^\circ_s$ = standard state volume change for solid phases of a reaction
$X_i$ = mole fraction of component i
$X_1$, $X_2$ = $X_{CO_2}$ values at lower limit ($X_1$) and upper limit ($X_2$) of integration
$\gamma_i$ = fugacity coefficient of component i

## EQUATIONS INVOLVING THE EQUILIBRIUM CONSTANT

Numerous workers have calculated T–$X_{CO_2}$ equilibria with equations derived from plots of experimental data on log K-1/T diagrams. A fundamental expression for isobaric equilibrium is:

$$\Delta G_r = 0 = \Delta G^\circ_r + RT \ ln\ K = \Delta H^\circ_r - T\Delta S^\circ_r + RT \ ln\ K \tag{1}$$

Rearranging:

$$ln\ K = -\frac{\Delta H^\circ_r}{R}\left(\frac{1}{T}\right) + \frac{\Delta S^\circ_r}{R} \tag{2}$$

If $\Delta H^\circ_r$ and $\Delta S^\circ_r$ are constant, this is a linear equation with slope equal to $-\Delta H^\circ_r/R$ and an intercept (at $1/T = 0$) of $\Delta S^\circ_r/R$. Assuming that no solid solutions are present, K may be expressed in terms of mole fractions of gas species. Thus, for a mixed-volatile reaction, an equilibrium

line fitted to experimental brackets plotted on a log $K_X$-1/T diagram provides an equation relating the mole fractions of gas species to temperature. As pointed out by Anderson (1970) some confusion in the equilibrium constant approach stems from the choice of the standard state. With equation (2) a "conventional" standard state as the pure phases (solids and gases) at 1 atm and T (standard state A of Anderson, 1970) has the advantage of comparing the derived enthalpy and entropy values with the 1 atm data in standard thermochemical tables (Robie and Waldbaum, 1968; Stull and Prophet, 1971) as well as introducing a consistency in the data of various workers. However, a choice of the standard state as the pure phase at P and T has the advantage of yielding enthalpy and entropy changes of reactions at elevated P–T conditions and, hence, direct comparison with the Clapeyron slope equation. We will now examine

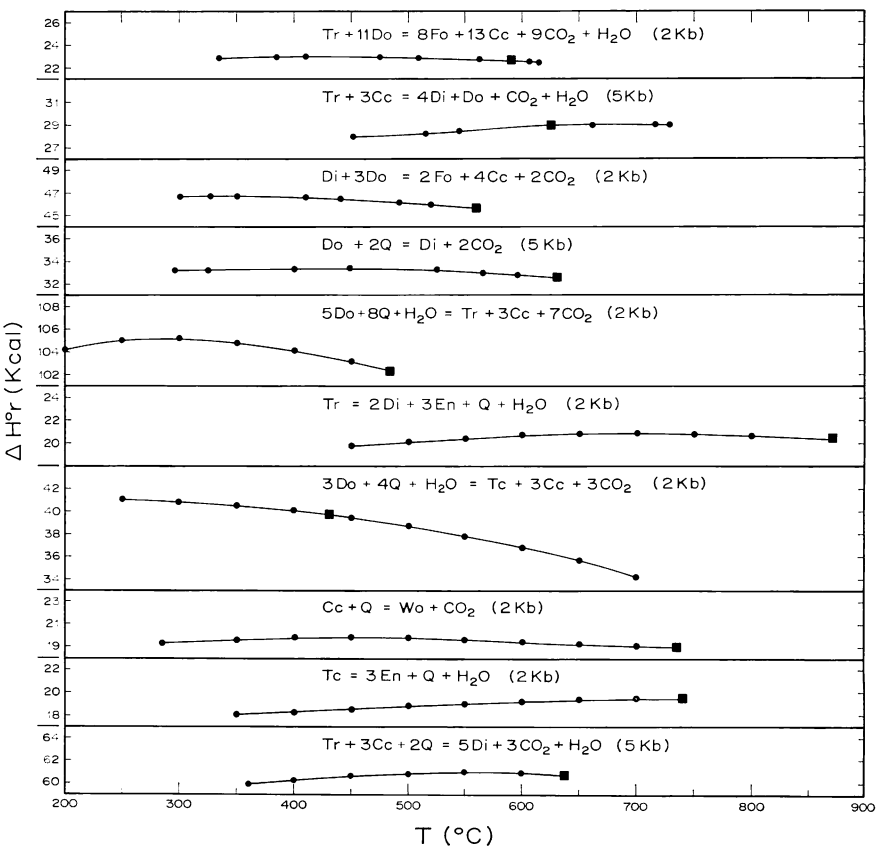


Fig. 1. Plot of $\Delta H^\circ_r$ as a function of temperature for selected equilibria, calculated with equations (3) and (4) in text. Filled square represents experimental equilibrium points from Skippen (1971), Greenwood (1967b), and from Slaughter, Kerrick, and Wall (1975), used for equation (3) in text.

various sources of uncertainty for equations derived from log K-1/T diagrams.

It has been assumed that equilibrium lines on log K-1/T diagrams are straight, implying that $\Delta H°_r$ and $\Delta S°_r$ are constant and independent of temperature. This assumption can be tested with the following method. First, the equilibrium constant ($K_2$) at any selected temperature ($T_2$) can be calculated using the relation:

$$RT_2 \ ln \ K_2 = \int_{T_1}^{T_2} \Delta S°_r dT + RT_1 \ ln \ K_1, \qquad (3)$$

where the lower limit of integration ($K_1$–$T_1$) is taken as the midpoint of

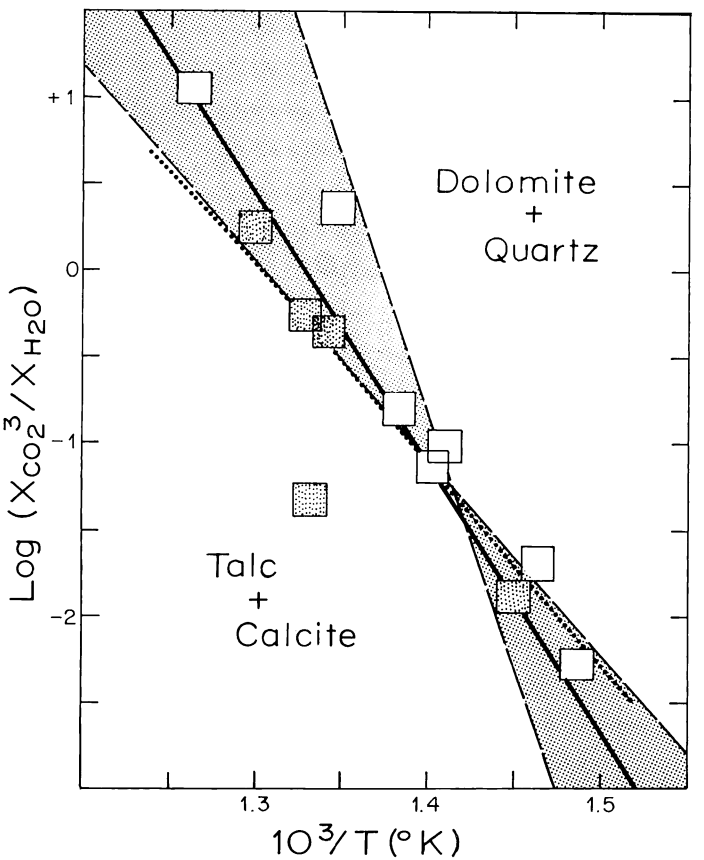


Fig. 2. Log K-1/T plot at 2 kb for the reaction: 3 dolomite + 4 quartz + $H_2O$ = talc + calcite + 3 $CO_2$. Experimental points are from Gordon and Greenwood (1970) and from Skippen (1971). Shaded band represents the total error in fitting an equilibrium line to the data points. The solid equilibrium line is that selected by Gordon and Greenwood (1970). The dotted line was calculated with equation (3) (text) from a starting point of 442°C and $X_{CO_2} = 0.4$.

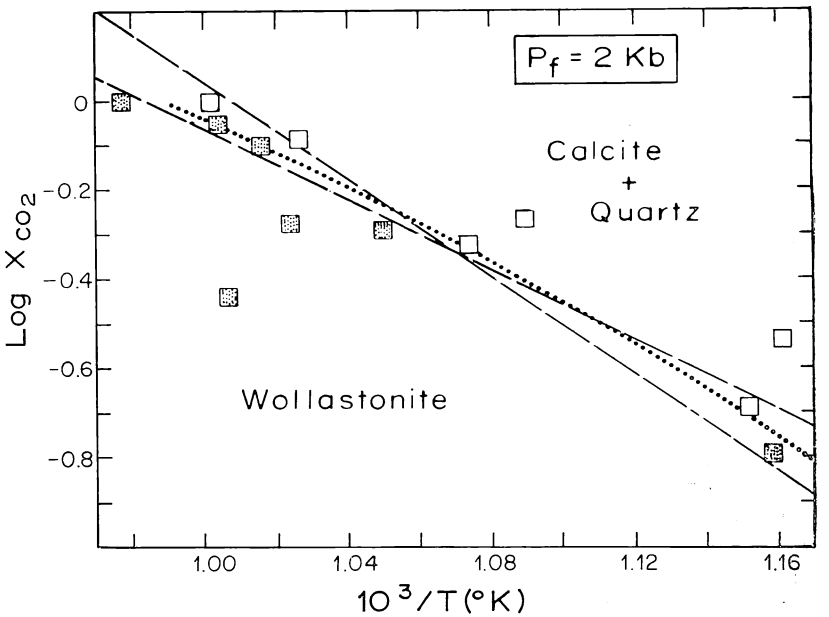


Fig. 3. Log K-1/T diagram for the reaction: calcite + quartz = wollastonite + $CO_2$, showing experimental data from Greenwood (1967b). The dotted line was calculated with equation (3) (text) from a starting point of 725°C, $X_{CO_2}$ = 1.0. The solid line represents the best fit of a straight equilibrium line through the midpoints of the experimental brackets.

an experimental equilibrium bracket. For such calculations we correct for non-ideal mixing in the fluid (using the data of Ryzhenko and Malinin, 1971), and the standard state is taken as unit activity of pure phases at P and T, such that the equilibrium constant is expressed in terms of activities of $H_2O$ and $CO_2$. This calculation involves an "exact" solution to the integral in equation 3 since $\Delta S°_r$ is adjusted for temperature change using high-temperature entropies of solids from Robie and Waldbaum (1968), of $H_2O$ from Burnham, Holloway, and Davis (1969), and of $CO_2$ calculated from Burnham and Wall (unpub.).[1] This then allows calculation of $\Delta H°_r$ at any temperature ($T_2$) from the relation:

$$\Delta H°_r = (T_2)\Delta S°_r - RT_2 \ln K_2 \qquad (4)$$

The results of such calculations for several mixed-volatile equilibria are shown in figure 1. For many equilibria shown, $\Delta H°_r$ varies by less than 0.5 kcal for a temperature range of 100°C. The reaction:

$$\text{dolomite} + \text{quartz} + H_2O = \text{talc} + \text{calcite} + CO_2,$$

shows the largest variation in $\Delta H°_r$; thus, comparing the equilibria shown in figure 1, this reaction would show the most curvature on a log K-1/T

[1] Details of P–T–$X_{CO_2}$ computer calculations and data sources are given in Slaughter, Wall, and Kerrick (1976).

diagram. However, as illustrated in figure 2, the calculated equilibrium line (dotted) shows little curvature. Considering that the temperature uncertainty of most experimental equilibrium brackets is at least ± 5°C, it would be virtually impossible to verify the curvature experimentally. In essence, a straight line will pass through the experimental brackets, as illustrated by the actual experimental data for this reaction plotted in figure 2. However, figure 3 provides an example of a reaction where widespread, narrow experimental brackets provide proof that the equilibrium line is *essentially* straight over an appreciable temperature range. Hence, the assumption of a straight-line relation of equilibria on log K-1/T diagrams leads to negligible error in the numerical solution of equilibrium constant expressions.

Since accurate fugacity data are available for *pure* $H_2O$ and $CO_2$ over a wide range of pressures and temperatures,[2] equilibrium constants can be calculated from two or more experimental equilibrium brackets of dehydration or decarbonation reactions, determined in the presence of pure $H_2O$ or pure $CO_2$, respectively. Such calculations are analagous to those of Anderson (1970) for the muscovite + quartz breakdown. Following this scheme, calculation of an equilibrium constant at a constant pressure of 2 kb, for example, could be accomplished through the following expression for a devolatilization reaction:

$$ln\ K = ln\ f_i^{n_i} = \frac{-\Delta H^\circ_r}{RT} + \frac{\Delta S^\circ_r}{R} - \frac{\Delta V_s\ (P\text{-}2000)}{RT} \qquad (5)$$

With two *narrow*[3] experimental brackets at widely-spaced temperatures, the only appreciable error in locating the equilibrium line on a log K-1/T plot arises from the error in $\Delta V_s$ in the last term on the far right of equation (5). The $\Delta V_s$ term is usually calculated with molar volume data at 1 atm and 25°C; however, a more accurate value would be calculated with compressibility and thermal expansion data for solid phases. Considering a practical example, one of the largest pressure corrections for the equilibrium constant is given by Chatterjee and Johannes (1974), who calculated the 1 atm equilibrium constant for muscovite decomposition by recalculating experimental equilibrium points from pressures as high as 8 kb (fig. 4). Because of the unusually large pressure correction, this reaction *may* provide an example of the maximum error introduced in the numerical solution of the equilibrium constant by neglecting the effect of P and T on $\Delta V_{solids}$. Compressibility and thermal expansion data[4] suggest that in the P–T range of the experimental data, $\Delta V_s$ for

[2] Fugacity data for $H_2O$ is given by Burnham, Holloway, and Davis (1969), and the fugacity of $CO_2$ up to 10 kb and 1000°C, computed from the P–V–T measurements of C. Wayne Burnham and V. J. Wall, is available through V. J. Wall of Monash University, Melbourne, Australia.

[3] We consider an equilibrium bracket to be "narrow" if determined within ± 5° to 10°C. An uncertainty less than ± 5°C is unlikely with conventional cold-seal vessels.

[4] Compressibilities were taken from Birch (1966), and thermal expansion data are from Skinner (1966). The thermal expansion of muscovite was assumed equal to that of pyrophyllite (data from Taylor and Bell, 1971).

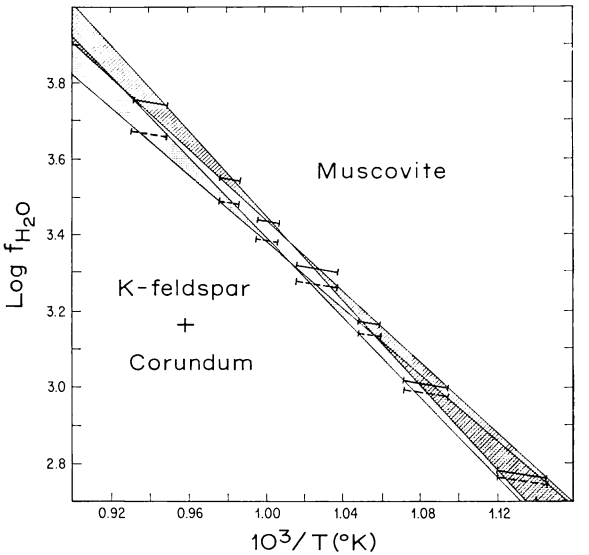


Fig. 4. Log K-1/T diagram at 1 atm for the upper stability of muscovite. Solid bars are equilibrium brackets from Chatterjee and Johannes (1974), whereas dashed bars are equilibrium brackets corrected for thermal expansion and compressibility of solid phases. The hachured area outlines the total error in fitting an equilibrium line through the solid bars, whereas the stippled area outlines the error in locating the equilibrium line through the dashed brackets.

this reaction may be about 0.5 cal/bar lower than the value at 25°C and 1 atm. Using equation (5) the equilibrium constant ($f_{H_2O}$) of this reaction was adjusted using the modified value of $\Delta V_s$, and the results are plotted in figure 4. The error band through the "corrected" brackets (stippled) overlaps that through the "uncorrected" brackets (hachured). Hence, for this reaction, correction for compressibility and thermal expansion provides no distinct improvement in the numerical solution (that is slope and intercept values) of the equilibrium constant. In essence, correction of the volume term is overshadowed by uncertainties in the experimental brackets. However, compared to experimental data for other equilibria, this reaction has particularly narrow experimental brackets over a wide range of P–T space. Thus, barring an equilibrium with an unusually large effect of changes in P and T on $\Delta V_s$, correction for compressibility and thermal expansion will not yield a significant improvement in the numerical solution of equilibrium constants from experimental data.

An important source of error in the equilibrium constants for reactions determined in volatile mixtures stems from errors in determining the fluid composition, within the experimental capsules, in the extremal ranges of $X_{CO_2}$. For example, with a two-volatile reaction:

$$ln\ K_X = ln\ X_{CO_2}^{n_{CO_2}} + ln\ X_{H_2O}^{n_{H_2O}},$$

it is clear that in the low-$X_{CO_2}$ range a large error in the term $ln\ X_{CO_2}^{n_{CO_2}}$ would be introduced by a small error in determination of the gas composition. A similar argument applies to the term $ln\ X_{H_2O}^{n_{H_2O}}$ in the high-$X_{CO_2}$ range. The importance of these errors is illustrated by Skippen and Hutcheon (1974) for the reaction:

$$3 \text{ magnesite} + 4 \text{ quartz} + H_2O = \text{talc} + 3\ CO_2,$$

where experimental data at $X_{CO_2} < 0.12$ and $X_{CO_2} > 0.92$ yield anomalous results on log K-1/T plots.

In published log K-1/T plots of equilibria determined in gas mixtures (Skippen, 1971, 1974; Gordon and Greenwood, 1970; Hewitt, 1973), ideal mixing has been assumed in the fluid phase, such that the fugacities of components in gas mixtures are derived through the Lewis and Randall rule. To examine the role of non-ideal mixing, consider the reaction:

$$3 \text{ dolomite} + 4 \text{ quartz} + H_2O = \text{talc} + 3 \text{ calcite} + 3\ CO_2$$

Taking the 1 bar-T standard state for the gas, the isobaric free energy change for this equilibrium is:

$$\begin{aligned}(\Delta G_r)_T^P &= \Delta H^\circ_r - T\Delta S^\circ_r + RT\ ln\ [(f^*_{CO_2})^3/(f^*_{H_2O})] \\ &= \Delta H^\circ_r - T\Delta S^\circ_r + RT\ ln\ [(\gamma_{CO_2} f^\circ_{CO_2} X_{CO_2})^3/(\gamma_{H_2O} f^\circ_{H_2O} X_{H_2O})]\end{aligned}$$

The term in brackets is defined as the equilibrium constant K. Separating the terms on the far right:

$$\begin{aligned}0 = \Delta H^\circ_r - T\Delta S^\circ_r + RT\ ln\ [(\gamma_{CO_2})^3/\gamma_{H_2O}] + \\ RT\ ln\ [(f^\circ_{CO_2} X_{CO_2})^3/f^\circ_{H_2O} X_{H_2O}]\end{aligned}$$

Defining the term in brackets on the far right as $K'_{id}$, and rearranging:

$$\log K'_{id} = -\frac{\Delta H^\circ}{2.303\ RT} + \left(\frac{\Delta S^\circ_r}{2.303\ R} - \log\ [(\gamma_{CO_2})^3/\gamma_{H_2O}]\right) \quad (6)$$

Thus, since $K'_{id}$ is plotted on published log $K_f$-1/T diagrams of mixed volatile equilibria, the term on the far right of equation (6) (that is, the "true" B term of the equilibrium constant) automatically incorporates departures from non-ideality. Assuming a straight-line relationship on a log K-1/T diagram thus implies that the ratio of the activity coefficients is a constant independent of temperature. Since the experimental brackets on this reaction (fig. 2) can accommodate either straight or curved lines, these brackets provide no test as to the validity of assuming a constant activity coefficient ratio. However, that this is a reasonable assumption is verified by the dotted line in figure 2, calculated using equation (3) with the equilibrium constant expressed in terms of *activities* of $CO_2$ and $H_2O$. This calculation thus adjusts for the change in activity coefficients

of $H_2O$ and $CO_2$ with changing temperature.[5]. In figure 2 the curvature of the calculated dotted line is minimal; hence, the straight-line assumption is reasonable for this equilibrium. However, the usual method of calculating this equilibrium constant at a pressure other than that of the experimental data does not account for the change in activity coefficients with changing pressure. For the reaction in figure 2, calculation of the equilibrium constant from the pressure of the experimental data ($P_1$) to a new pressure ($P_2$) involves:

$$\log\ (K)_{P_2} = \log\ [(\gamma_{CO_2}\ f^\circ_{CO_2}\ X''_{CO_2})^3 / (\gamma_{H_2O}\ f^\circ_{H_2O}\ X''_{H_2O})]_{P_2}$$
$$= -\frac{\Delta H^\circ_r}{2.303\ RT} + \frac{\Delta S^\circ_r}{2.303\ R} - \frac{\Delta V_s(P_2 - P_1)}{2.303\ RT} \qquad (7)$$

Assuming ideal mixing, as in the case of published log K-1/T diagrams of mixed-volatile equilibria, such pressure correction would yield the term:

$$\log\ (K'_{id})_{P_2} = \log\ [(f^\circ_{CO_2}\ X'_{CO_2})^3/(f^\circ_{H_2O}\ X'_{H_2O})]_{P_2} \qquad (8)$$

At selected temperatures, data for the activity coefficients and fugacities of $H_2O$ and $CO_2$[6] allow calculation of $X''_{CO_2}$ and $X''_{H_2O}$ which would satisfy $(K)_{P_2}$ in equation (7). From these values, the resultant "corrected" ideal equilibrium constant ($K''_{id}$) is then calculated from:

$$\log\ (K''_{id})_{P_2} = \log\ [(f^\circ_{CO_2}\ X''_{CO_2})^3/(f^\circ_{H_2O}\ X''_{H_2O})]$$

Using the solid line on figure 2 as a base, equilibrium constants for equations (7) and (8) were calculated for selected temperatures at 0.5 kb and at 1 kb. The respective values of $X'_{CO_2}$ and $X''_{CO_2}$ at each pressure permit construction of the T–$X_{CO_2}$ diagram (fig. 5A). For this equilibrium it is clear that there is a significant difference in location of the uncorrected (dashed) versus corrected (solid) curves at each pressure. Figure 5B shows the results of analagous calculations for a higher-temperature equilibrium. As expected, the difference in location of the corrected and uncorrected curves is not as significant as for the lower-temperature reaction shown in figure 5A. However, we recommend correction for the change in activity coefficients with changing pressure for all equilibria in the pressure range (<2kb) where activity data exist for $H_2O$–$CO_2$ mixtures.

Perhaps the most important source of error in determining equilibrium constants from log K-1/T plots stems from the total uncertainty in fitting the equilibrium line to the plotted experimental data. This source of uncertainty is illustrated in the study of Skippen (1971, 1974) who has plotted his experimental data on log K-1/T diagrams, from which he derived equations of the form:

$$\log\ K_f = \frac{A}{T} + B + \frac{C\ (P_{total} - 2000)}{T}\ , \qquad (9)$$

[5] For some readers it may be useful to note that Ryzhenko and Malinin's (1971) data, used in calculating activities of $H_2O$ and $CO_2$, is based on Franck and Tödheide's (1959) experimentally-determined compressibility data which was obtained over a temperature range of 400° to 750°C and pressures from 0.3 to 2 kb.

[6] Data sources are discussed in Slaughter, Wall, and Kerrick (1976).

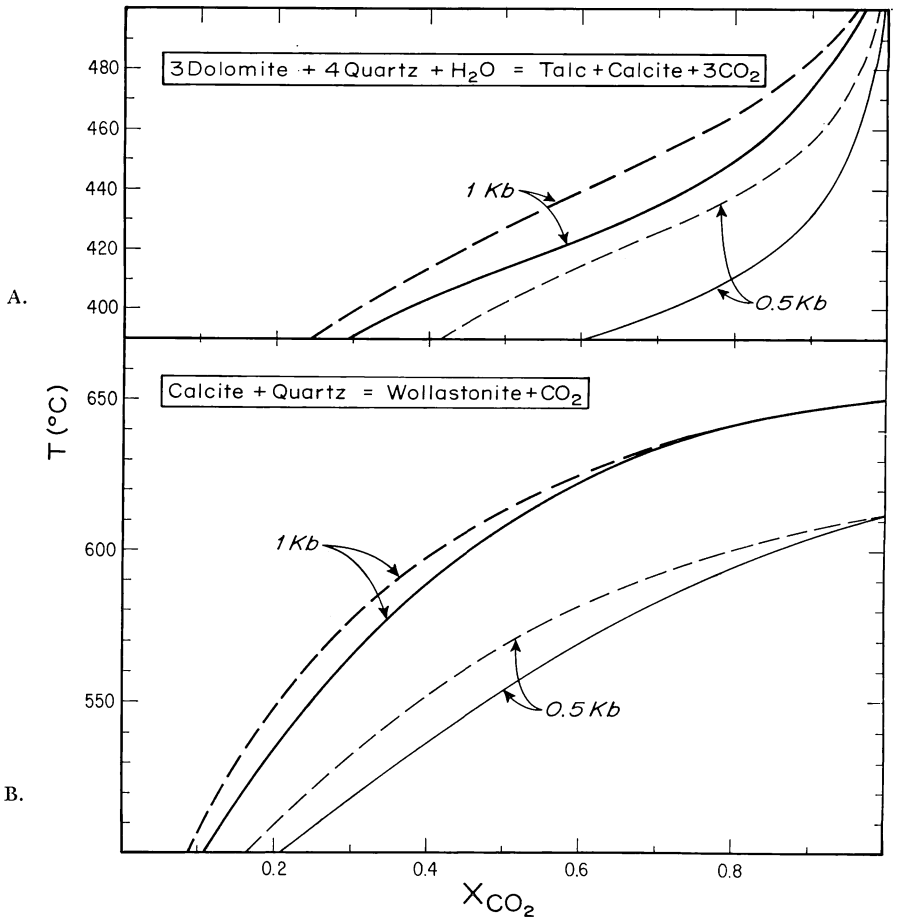


Fig. 5. T–X diagrams calculated from log K expressions derived from experimental data at 2 kb. The dashed lines were calculated assuming that the activity coefficients of gas species remain constant with changing pressure [eq 8], whereas the solid curves were derived by correcting for the change in activity coefficients with changing pressure [eq 7]. (A) was calculated using the solid line in figure 2 as a base, whereas (B) was calculated starting with the solid line in figure 3.

which were then used for the construction of isobaric T–X equilibria in the system CaO–MgO–SiO–$H_2O$–$CO_2$. Here, the equilibrium constant is expressed by the *fugacities* of the gas species at P and T and, hence, is equivalent to standard state C of Anderson (1970).[7] As in equation (5), the term on the far right in equation (9) is a correction for experimental data obtained at pressures other than 2000 bars. Skippen (1971) experimentally determined five reactions and, for each reaction, derived expressions for the A and B constants in equation (9) from log K-1/T dia-

[7] Anderson's (1970) standard state C refers to the pure solid phases at T and 2000 bars and the ideal pure gas at T and 1 bar.

grams. Through the appropriate coupling of these five reactions he derived constants in equation (9) for 44 other equilibria within the "siliceous dolomite" system. Skippen (1974) has carefully analyzed the uncertainties introduced in such derivations. Most of the uncertainties in the T–X locations of equilibria presented by Skippen (1971, 1974) are introduced by two of the five "key" reactions:[8]

$$\text{talc} = 3 \text{ enstatite} + \text{quartz} + H_2O \qquad [1]$$

$$4 \text{ talc} + 5 \text{ dolomite} = 5 \text{ diopside} + 6 \text{ forsterite} + 10\ CO_2 + 4\ H_2O \qquad [5]$$

The numbers of these equilibria correspond to those of Skippen (1971, 1974). The uncertainty in the equilibrium constant for reaction [1] is illustrated in figure 6. Lines of minimum and maximum slope are drawn (dashed lines) which yield the respective uncertainty limits of −5729 and −11428 for the A constant, and 8.777 and 14.586 for the B constant.[9] These uncertainties are somewhat larger than those tabulated by Skippen (1974, table 2). Clearly, there is no particular preference for any line constrained by the experimental data, such that the extremal lines yielding the limits of uncertainty are no less probable than any other lines of intermediate slope. Hence, there is no preference for a "most probable" value (or range of values) for the A and B constants within the uncertainty limits stated above.[10] An argument similar to the above accounts for much of the uncertainty in the A and B constants of reaction [5] (see Skippen, 1974, table 2).[11] Aside from one reaction (Skippen's reaction [4]), all equilibria on his T–X diagrams were derived from coupling the equilibrium constants for reaction [1] and/or reaction [5], thus accounting for much of the uncertainty in location of equilibria on his T–X diagrams (see fig. 5 of Skippen, 1974). These large uncertainties emphasize the need for precise experimental brackets for equations of state derived *solely* from phase equilibrium experiments.

We conclude that the equilibrium constant approach can yield accurate equations for extrapolating equilibria in P–T–$X_{CO_2}$ space *if* two or more narrow experimental equilibrium brackets are available at wide-

[8] In Skippen's 1974 paper, all equilibria involving dolomite have been recast in terms of calcite and magnesite; for example, Skippen (1974) expresses the reaction:

$$8 \text{ quartz} + 5 \text{ dolomite} + H_2O = \text{tremolite} + 3 \text{ calcite} + 7\ CO_2,$$

as:

$$8 \text{ quartz} + 5 \text{ magnesite} + 2 \text{ calcite} + H_2O = \text{tremolite} + 7\ CO_2$$

[9] This type of error analysis is identical to that illustrated by Chernosky (1974) for his experimental data on cordierite equilibria.

[10] Note that the uncertainties in the A and B constants are not independent. For example, selection of the most negative possible value of the A constant (—11,428) requires the most positive value of the B constant (14.586).

[11] Additional uncertainty in the equilibrium constant for reaction [5] stems from the error in the free energy of the reaction:

$$\text{calcite} + \text{magnesite} = \text{dolomite},$$

which Skippen (1974) coupled to the equilibrium constant for reaction [5] from Skippen (1971).

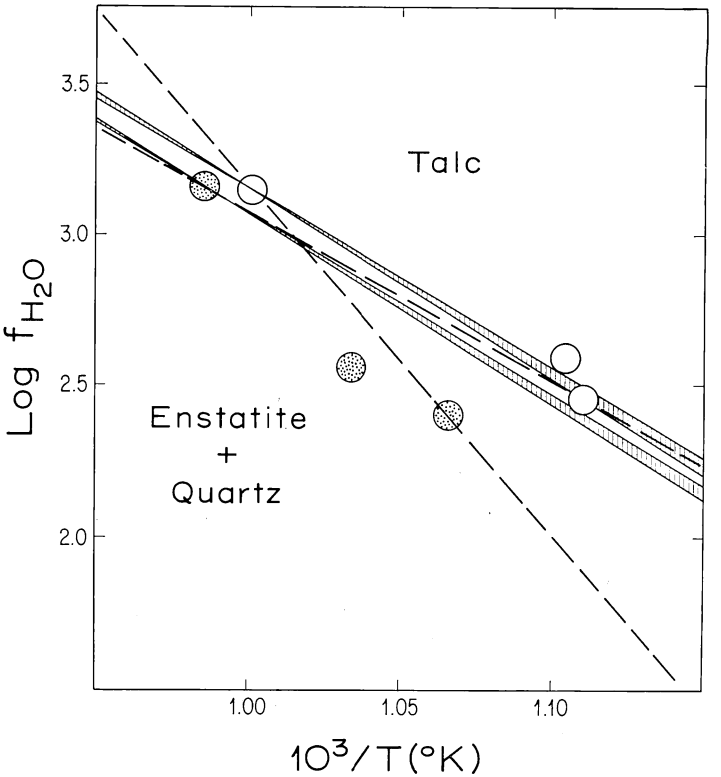


Fig. 6. Log K-1/T diagram at $P_f = 2$ kb showing Skippen's (1971) experimental data for the reaction: talc = 3 enstatite + quartz + $H_2O$. Open circles: talc stable; stippled circles: enstatite + quartz stable. Dashed lines outline the maximum error in fitting an equilibrium line to the experimental data points. Solid lines were extrapolated from the experimental bracket at log K $\cong$ 3.1. Hachured bands are error limits for lines extrapolated from the limits of this experimental bracket, by calculating the total uncertainty in $\Delta S°_r$ (see text).

spread temperatures. This point is elaborated in the last section of this paper.

## EQUATIONS FOR EXTRAPOLATION FROM AN EXPERIMENTAL EQUILIBRIUM BRACKET

*Greenwood's equation.*—Greenwood (1967a) has derived the following equation for extrapolating equilibria on *isobaric* $T\text{–}X_{CO_2}$ diagrams:

$$-\frac{1}{T} = A + \frac{R}{\Delta H°_r}\left[n_{CO_2}\ ln\ X_{CO_2} + n_{H_2O}\ ln\ X_{H_2O}\right], \qquad (10)$$

where A is the integration constant evaluated at the starting point (usually an experimental equilibrium bracket). To derive an equivalent expression involving reaction entropy, we differentiate equation (1) at constant pressure:

$$d(\Delta G_r)_P = 0 = RT\ d\ ln\ K + R\ ln\ K\ dT - \Delta S°_r\ dT \qquad (11)$$

Expressing the equilibrium constant in terms of mole fractions and rearranging:

$$0 = RT\ d\ ln\ [X_{CO_2}^{n_{CO_2}} \cdot X_{H_2O}^{n_{H_2O}}] + [-\Delta S^\circ_r + n_{CO_2}\ R\ ln\ X_{CO_2} + n_{H_2O}\ R\ ln\ X_{H_2O}]\ dT$$

Integrating between the respective lower and upper limits $T_1$-$X_1$ and $T_2$-$X_2$,[12] cancelling terms, and rearranging:

$$\Delta S^\circ_r\ T_2 - n_{CO_2}\ RT_2\ ln\ X_2 - n_{H_2O}\ RT_2\ ln\ (1\text{-}X_2) = \Delta S^\circ_r\ T_1 - n_{CO_2}\ RT_1\ ln\ X_1 - n_{H_2O}\ RT_1\ ln\ (1\text{-}X_1) \quad (12)$$

Designating the term on the right side of eq 12 as the integration constant B and rearranging:

$$\frac{1}{T_2} = [\Delta S^\circ_r - n_{CO_2}\ R\ ln\ X_2 - n_{H_2O}\ R\ ln\ (1-X_2)]/B \quad (13)$$

For equation (10), estimates of $\Delta H^\circ_r$ can be obtained from either the slope of an equilibrium line on a log K-1/T plot or from calculations using high-temperature entropies.

If $\Delta H^\circ_r$ is to be derived from log K-1/T diagrams, it is imperative that K be expressed in terms of mole fractions of gas components rather than fugacities. This conclusion is evident since equation (10) can be readily derived from the well-known Van't Hoff equation:

$$\frac{d\ (ln\ K_X)}{dT} = \frac{d\ ln\ [X_{CO_2}^{n_{CO_2}} \cdot X_{H_2O}^{n_{H_2O}}]}{dT} = \frac{\Delta H^\circ_r}{RT^2}$$

For this purpose it is unfortunate that the equilibrium constant in most published log K-1/T diagrams is expressed in terms of fugacities of gas components. Anderson (1970) has clearly outlined the various equilibrium constants (that is, various standard states) and corresponding values for $\Delta H^\circ_r$.

The uncertainty in $\Delta H^\circ_r$ derived from log K-1/T diagrams is dependent upon the precision uncertainties in the experimental brackets. Where there are two or more widespread, narrow experimental brackets, there will be little error in $\Delta H^\circ_r$, thus introducing little uncertainty in T–X extrapolations using equation (10). In contrast, large uncertainties in T–X extrapolations using this equation result where wide experimental brackets yield a correspondingly large error in $\Delta H^\circ_r$. These conclusions can be illustrated by comparing T–X extrapolations for the following reactions:

$$\text{talc} = \text{enstatite} + \text{quartz} + H_2O$$

$$\text{calcite} + \text{quartz} = \text{wollastonite} + CO_2$$

[12] For some readers it should be noted that $\Delta G_r$ is a state function, so that integration of the function $d(\Delta G_r)_P$ is independent of the integration "path".

The data in figure 6 and in figure 3 were plotted on log $K_X$-1/T diagrams, and, for each reaction, the limiting lines through the experimental brackets yielded minimum and maximum values for $\Delta H°_r$. The extremal values of $\Delta H°_r$ were then used in equation (10) to yield the corresponding upper and lower uncertainty limits for the extrapolated T–X curves, as shown in figure 7. It is clear that the excellent experimental control for the wollastonite reaction [see fig. 3] leads to little uncertainty in the T–X extrapolation, whereas the lack of two or more narrow experimental brackets for the talc reaction [see fig. 6] results in a large uncertainty in the extrapolated T–X curve for this equilibrium.

For an experimental point determined in gas mixtures, $\Delta H°_r$ for use in equation (10) can be calculated with:

$$\Delta H°_r = T\Delta S°_r - RT \ ln \ K_X \qquad (14)$$

For dehydration or decarbonation reactions involving $H_2O$ or $CO_2$, respectively, a convenient starting point for T–X extrapolation is the equilibrium determined in the presence of pure gas species. Here the reaction

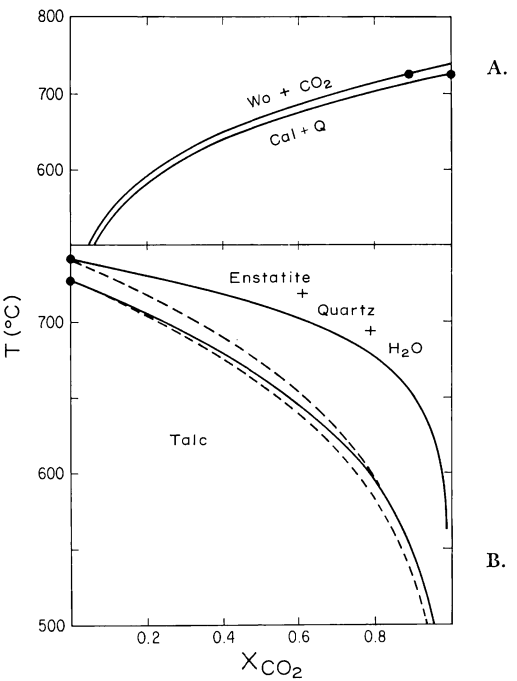


Fig. 7. T–X diagrams calculated with Greenwood's expression (eq 10 in text). Each diagram shows two solid curves which were calculated from the maximum and minimum $\Delta H°_r$ derived from the corresponding extremal slopes on an equilibrium line fit to experimental data on a log $K_x$-1/T diagram. See text for details. Filled circles represent limiting experimental points from Greenwood (1967b) for (A) and from Skippen (1971) for (B). Dashed lines were calculated with equation (19) in text.

enthalpy is readily calculated with $\Delta S^\circ_r$ since, in the presence of the pure gas species:

$$\Delta H^\circ_r = T\Delta S^\circ_r \tag{15}$$

Because this type of calculation shares the same data source as the equations to be discussed next, evaluation of T–X extrapolations based on high-temperature entropies will be discussed together in the next section.

*Equations using free energies of $CO_2$ and $H_2O$.*—To include the pressure effect on free energy we may reformulate and differentiate equation (1) as:

$$d\Delta G_r = 0 = \Delta V^\circ_r \, dP - \Delta S^\circ_r \, dT + d(RT \; ln \; K) \tag{16}$$

Integrating:[13]

$$\Delta\Delta G_r = 0 = \int_{P_1}^{P_2} \Delta V^\circ_r \, dP - \int_{T_1}^{T_2} \Delta S^\circ_r \, dT + RT_2 \; ln \; K_2 - RT_1 \; ln \; K_1 \tag{17}$$

Expanding the terms $\Delta V^\circ_r$ and $\Delta S^\circ_r$:

$$\Delta\Delta G_r = 0 = \int_{P_1}^{P_2} \Delta V^\circ_s \, dP + n_{CO_2} \int_{P_1}^{P_2} V_{CO_2} \, dP + n_{H_2O} \int_{P_1}^{P_2} V_{H_2O} \, dP$$
$$- \int_{T_1}^{T_2} \Delta S^\circ_s \, dT - n_{CO_2} \int_{T_1}^{T_2} S_{CO_2} \, dT$$
$$- n_{H_2O} \int_{T_1}^{T_2} S_{H_2O} \, dT + RT_2 \; ln \; K_2 - RT_1 \; ln \; K_1$$

Since:

$$n_i \int_{P_1}^{P_2} V_i \, dP - n_i \int_{T_1}^{T_2} S_i \, dT = n_i \, (G_i)_{T_2}^{P_2} - n_i \, (G_i)_{T_1}^{P_1},$$

then:

$$\Delta\Delta G_r = 0 = \int_{P_1}^{P_2} \Delta V^\circ_s \, dP - \int_{T_1}^{T_2} \Delta S^\circ_s \, dT + n_{H_2O} \left[ (G_{H_2O})_{T_2}^{P_2} - (G_{H_2O})_{T_1}^{P_1} \right]$$

[13] For some readers it will be useful to note that an entropy of mixing term does not appear in equation (17). The term: $RT_2 \; ln \; K_2 — RT_1 \; ln \; K_1$, can be readily derived by differentiation of the term RT *ln* K in equation (16) as the product of two variables (T and K), and then integration (by parts) of the result between the limits $T_1$-$K_1$ and $T_2$-$K_2$. As in the derivation of equation (12), the final result is independent of the path taken for the integration.

$$+ n_{H_2O} \left[RT_2 \ln (X_{H_2O})_{T_2}^{P_2} - RT_1 \ln (X_{H_2O})_{T_1}^{P_1}\right]$$

$$+ n_{CO_2} \left[(G_{CO_2})_{T_2}^{P_2} - (G_{CO_2})_{T_1}^{P_1}\right]$$

$$+ n_{CO_2} \left[RT_2 \ln (X_{CO_2})_{T_2}^{P_2} - RT_1 (X_{CO_2})_{T_1}^{P_1}\right] \quad (18)$$

For non-ideal gas mixtures, the mole fractions would be replaced by activities, yielding equation (1) of Slaughter, Kerrick, and Wall (1975). The equation for *isobaric* extrapolations, readily derived from equation (18) (see Slaughter, Kerrick, and Wall, 1975, p. 153), is:

$$0 = -\int_{T_1}^{T_2} \Delta S^\circ_s \, dT + n_{H_2O} \left[(G_{H_2O})_{T_2}^{P} - (G_{H_2O})_{T_1}^{P}\right]$$

$$+ n_{H_2O} \left[RT_2 \ln (1\text{-}X_2) - RT_1 \ln (1\text{-}X_1)\right]$$

$$+ n_{CO_2} \left[(G_{CO_2})_{T_2}^{P} - (G_{CO_2})_{T_1}^{P}\right]$$

$$+ n_{CO_2} \left[RT_2 \ln X_2 - RT_1 \ln X_1\right] \quad (19)$$

Replacing activities for mole fractions (that is, going from ideal gas mixtures to real gas mixtures) we arrive at equation (2) of Slaughter, Kerrick, and Wall (1975). At the Pennsylvania State University, we have developed interactive (A.P.L.) computer programs for P–T–$X_{CO_2}$ extrapolations according to equations (18) and (19) (Slaughter, Wall, and Kerrick, 1976). In this paper, all extrapolations with these equations were made using molar volume data from Robie, Bethke, and Beardsley (1967), high temperature entropies from Robie and Waldbaum (1968), $H_2O$ free energy from Burnham, Holloway, and Davis (1969), and $CO_2$ free energy computed from data of Burnham and Wall (unpub.). Since *both* thermal expansion and compressibility data are lacking for all solid phases in most equilibria, our calculations are usually made with $\Delta V_s$ calculated from 25°C, 1 atm data.[14] However, equations (18) and (19) provide good agreement between experimental equilibrium brackets at widely-spaced P–T points (Wall and Essene, 1972; Kerrick, Hunt, and Wall, 1973; Slaughter, Kerrick, and Wall, 1975); thus, correction for compressibility and thermal expansion is relatively unimportant in most cases.

Equation (19) is essentially a reformulation of equation (13). The difference between these equations arises from the fact that equation (19) represents an "exact" solution, since it accounts for the change in en-

[14] Our computer program used in P–T–$X_{CO_2}$ extrapolations (Slaughter, Wall, and Kerrick, 1976) has the option to consider thermal expansion and compressibility of solid phases.

tropies of solids[15] and gases with changing temperature, whereas equation (13) assumes that $\Delta S°_r$ is constant, having the value at the lower limit of integration.

*Isobaric T–X extrapolations.*—With figures 8 and 9, we now examine the *isobaric* T-X extrapolations of various equilibria to intercompare the results of equation (10) (Greenwood's expression) with that of equation (19) for both ideal and non-ideal fluid mixing. Note that in all these figures, the dashed lines were calculated with equation (10) using $\Delta H°_r$ calculated with equation (14) or (15), the dotted line was calculated with equation (19) assuming ideal mixing, and the solid lines were calculated with equation (19) correcting for non-ideal fluid mixing from data of Ryzhenko and Malinin (1971).

First, we will examine the T–X extrapolation of a mixed-volatile equilibrium in the high-temperature range (fig. 8), where the importance of non-ideal mixing in the fluid will be minimal. Error introduced by precision uncertainty in the thermochemical data,[16] illustrated by the two dashed and two solid lines, is of minor importance. Note that the curves extrapolated with equation (19) assuming ideal mixing are virtually identical to that calculated with equation (10). This reflects the fact that there is little variation in $\Delta S°_r$ (and $\Delta H°_r$) with temperature, a point previously discussed with the aid of figure 1. Consequently, Greenwood's "constant enthalpy" expression (eq 10) is quite adequate for extrapolations assuming ideal mixing. We also note that the solid curves, which were calculated with equation (19) correcting for non-ideal gas mixing, are quite close to those for ideal mixing. Thus, as expected, correction for non-ideality is unimportant for T–X extrapolations of equilibria in the high-temperature range (>500°C). All extrapolated curves in figure 8 fit Greenwood's narrow experimental brackets, such that, for small departures from ideal fluid mixing, experimental confirmation of the activity-corrected curve is not feasible (see also Greenwood, 1967b, p. 1671-1672).

Figure 9 illustrates an extrapolation in the low-temperature range where non-ideal mixing will be most important. As in figure 8, equation (10) gives results identical to that of equation (19) for ideal fluid mixing; furthermore, the errors resulting from precision uncertainties in the thermochemical data are rather small. However, there is a significant difference between the solid curves, corrected for non-ideal mixing, and those extrapolated with the assumption of ideal mixing. Note that the "activity-corrected" curve fits the experimental brackets, whereas the "ideal" curves are well outside these brackets. Thus, for equations using

[15] The change in $\Delta S°_s$ with temperature is accomplished by polynomials fit to Robie and Waldbaum's (1968) high-temperature entropy data (see Slaughter, Kerrick, and Wall, 1975, p. 153).

[16] Uncertainty in $\Delta S_s$ was calculated by summing the uncertainty in the entropies of solid phases as given by Robie and Waldbaum (1968), and uncertainty in the entropy and free energy of $H_2O$ is from Burnham, Holloway, and Davis (1969). Uncertainty in the entropy and free energy of $CO_2$ was arbitrarily taken as three times that of $H_2O$.

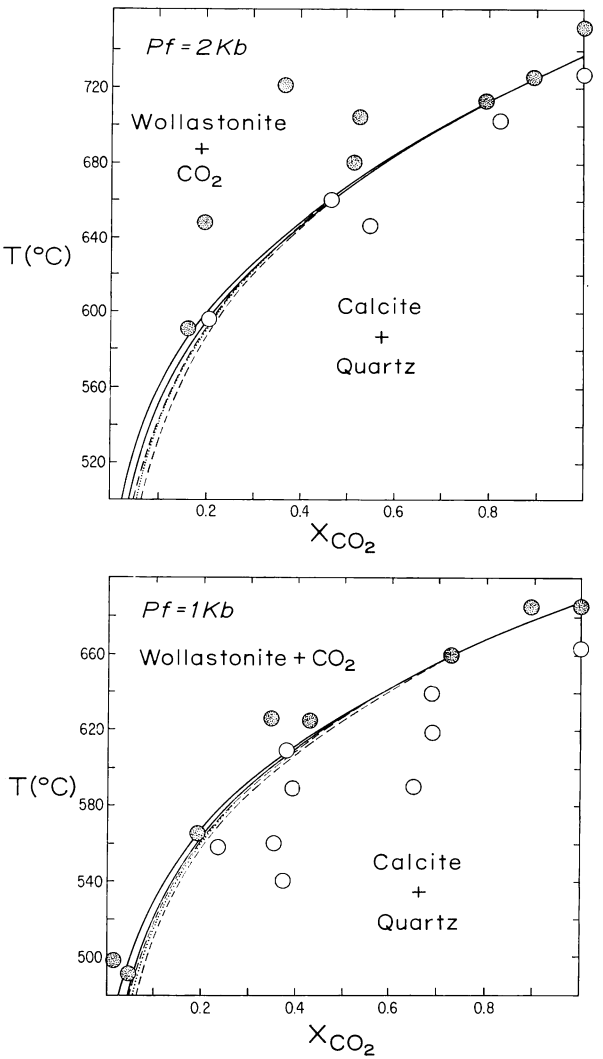


Fig. 8. T–$X_{CO_2}$ diagrams for the reaction: calcite + quartz = wollastonite + $CO_2$, showing experimental data of Greenwood (1967b). Stippled circles: wollastonite stable; open circles: calcite + quartz stable. Curves were extrapolated from points at $X_{CO_2}$ = 1.0. The solid curves were calculated with equation (19) assuming non-ideal gas mixing, the dotted curve was calculated with equation (19) assuming ideal gas mixing, and the dashed curves were calculated with equation (10). The two sets of solid and dashed curves were calculated from the maximum and minimum uncertainties in $S°_r$ (see text). For graphical clarity, two sets of curves (that is, error estimates) are not shown for the dotted curve.

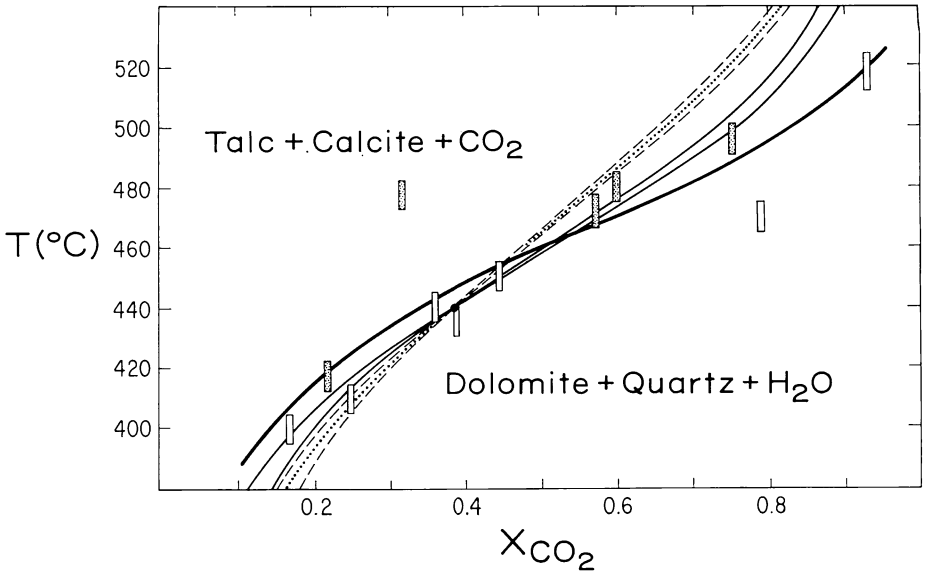


Fig. 9. T–$X_{CO_2}$ diagram at $P_f$ = 2 kb showing experimental data from Gordon and Greenwood (1970) and from Skippen (1971). Open rectangles: dolomite + quartz stable; stippled rectangles: talc + calcite stable. The heavy solid curve is from Gordon and Greenwood (1970). Symbols for other equilibrium lines are explained in figure 8.

high-temperature data, this example provides experimental verification of the necessity to correct for non-ideal mixing for T–X extrapolations in the low-temperature range.

In figure 9 the heavy solid line was calculated by Gordon and Greenwood (1970) who extrapolated this curve with equation (10) using a starting point of 447°C and $X_{CO_2}$ = 0.4. The $\Delta H°_r$ for this calculation was derived from the slope of the equilibrium line fit to a log K-1/T plot of their experimental data. Since there is reasonably good experimental control for this reaction over a range of T–X space, then this procedure has the advantage of *insuring* thermodynamic self-consistency of the extrapolated T–X curve.[17] Since we can routinely activity-correct extrapolations with equation (19) (see Slaughter, Wall, and Kerrick, 1976), there is no major advantage in using the log K-1/T approach compared to equation (19) correcting for non-ideality. However, for mixed-volatile equilibria experimentally determined outside of the range of Ryzhenko and Malinin's (1971) activity data for $H_2O$–$CO_2$ mixtures, derivation of equations from log K-1/T diagrams is advised providing that: (A) the experimental data was obtained at the pressure of the resulting T–X diagram, and (B) more than one precise experimental bracket is available.

Strong departures from ideal mixing at high pressures could seriously affect extrapolations using equation (19). However, for the 6 kb equi-

[17] As previously discussed such thermodynamic self consistency is only guaranteed for experimental data obtained at the same pressure as the isobaric T–X extrapolation.

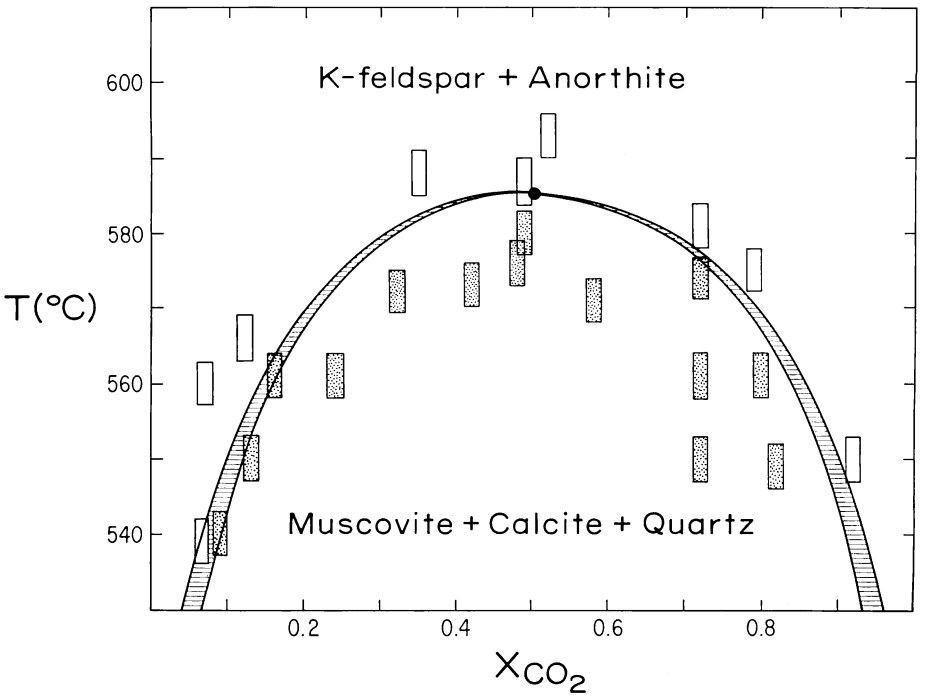


Fig. 10. T–$X_{CO_2}$ diagram at $P_f$ = 6 kb, showing experimental data from Hewitt (1973). Stippled rectangles: muscovite + calcite + quartz stable; open rectangles: K-feldspar + anorthite stable. The filled circle is the starting point for extrapolations using equation (19) assuming ideal mixing in the fluid. The hachured area illustrates the error in the extrapolation arising from the uncertainty in $\Delta S°_r$ (see text).

librium shown in figure 10, the curve extrapolated assuming ideal mixing provides an adequate fit to the experimental data. This agreement, however, may not be particularly meaningful since: (A) only one *narrow* equilibrium bracket was obtained (at T $\cong$ 540°C), and (B) variations in Al/Si order-disorder in alkali feldspar and in muscovite will affect the positions of the extrapolated curves.[18] We will now discuss this latter problem in more detail.

An additional source of uncertainty in extrapolations using high-temperature entropies concerns the configurational entropies of phases having cation disorder, a notorious problem with many aluminum silicates. For example, the configurational entropies of maximum microcline and high sanidine may differ by 4.5 cal/mol°K.[19] Kerrick (1974)

[18] The curves in figure 10 were extrapolated using entropy data for muscovite and high sanidine from Robie and Waldbaum (1968). However, the entropy of muscovite as given by Robie and Waldbaum (1968) may be low by several entropy units (Kerrick, 1974, p. 755).

[19] This difference in configurational entropy assumes no adherence to the "aluminum avoidance principle" (Kerrick and Darken, 1975).

has shown how the difference in configurational entropy between microcline and high sanidine affects the T–X extrapolations of the reaction:[20]

$$\text{muscovite} + \text{quartz} = \text{andalusite} + \text{K-feldspar} + H_2O$$

Crystallographic studies of tetrahedral ordering as a function of temperature, such as exists for albite, are necessary for refined extrapolations of mixed-volatile equilibria. An example of such refinement may be illustrated for the reaction:

$$\text{paragonite} = \text{albite} + \text{corundum} + H_2O$$

From the tetrahedral site fractionation of Al and Si as a function of temperature (Smith, 1974, p. 77), a configurational entropy can be calculated from:

$$\Delta S_{cfg} = -R\,[X_{A1}\,ln\,X_{A1} + (1\text{-}X_{A1})\,ln\,(1\text{-}X_{A1})] - 3R\,[X'_{A1}\,ln\,X'_{A1} + (1\text{-}X'_{A1})\,ln\,(1\text{-}X'_{A1})],$$

where $X_{A1}$ is the fractional occupancy of Al in the $T_1(0)$ site, and $X'_{A1}$ is the fractional occupancy in the other three sites [$T_1$ (m), $T_2$ (0), and $T_2$ (m)]. For a series of temperatures between 400° and 1100°C the calculated $\Delta S_{cfg}$ was added to the entropy of low albite given by Robie and Waldbaum (1968) to yield an "intermediate" albite entropy corrected for Al–Si order-disorder. The importance of considering albite order-disorder in T–X extrapolations is illustrated in figure 11, where there are significant differences in the extrapolated T–X equilibria of the various albites. Further refinement in this extrapolation would necessitate knowing Al–Si ordering in paragonite. Obviously, there is a clear need for determining the equilibrium Al–Si ordering as a function of temperature. However, Al–Si order-disorder may not be a particularly serious problem when we consider uncertainty in experimental brackets. For example, experimental uncertainty in the equilibrium brackets for muscovite decomposition, shown in figure 12, are typical of conventional hydrothermal experiments. Using equation (18), three curves have been extrapolated from the narrowest (6kb) bracket, each for a different combination of Al–Si disorder in coexisting muscovite and K-feldspar. Note that *all* curves pass through the experimental brackets such that the experimental data shed no light on the state of disorder of the experimental products. In essence, correction for cation disorder is overshadowed by the uncertainty in the experimental brackets. Fortunately, phases in the system CaO–MgO–$SiO_2$–$CO_2$–$H_2O$, which contains numerous mixed-volatile equilibria of geologic interest, do not have cation order-disorder (Sueno and others, 1973; Cameron and others, 1973).[21]

[20] Since most experimental brackets for the muscovite + quartz breakdown reaction involve high sanidine, a curve extrapolated for the disordered polymorph would be relevant to most experimental data. However, for interpreting metamorphic conditions the experimental P–T–$X_{CO_2}$ curves must be adjusted for the structural state of the feldspar occurring in natural systems.

[21] Disorder in dolomite occurs at temperatures ($\geqq$ 1000°C) above the range of most metamorphic systems (Goldsmith and Heard, 1961).

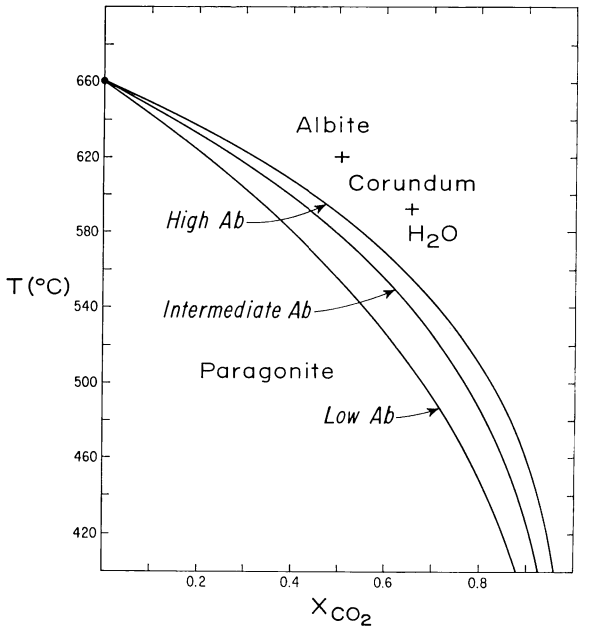


Fig. 11. T–$X_{CO_2}$ diagram at $P_f$ = 7 kb showing dependence of the extrapolated paragonite breakdown reaction on the Al/Si order-disorder of albite. "Intermediate" albite is explained in text.

A remaining problem with determining the entropies of phases stems from the lack of heat capacity measurements over the entire temperature range of interest. For the system CaO–MgO–$SiO_2$–$CO_2$–$H_2O$, which is of primary interest in this paper, heat capacities of several phases (calcite, dolomite, tremolite, and talc) have been measured down to temperatures of 10° to 15°K. For these phases, the entropy error introduced in the third-law extrapolation to 0°K would be very small. However, heat capacities for dolomite, tremolite, and talc have been measured up to only 300°K, so that the high-temperature entropies of these phases are based on Maier-Kelley heat capacity equations extrapolated from the low-temperature measurements. As pointed out by Robie and Stout (1963) the Maier-Kelley expression provides an excellent fit of the heat capacities in the higher temperature range of measurement, so this function should provide a reasonable extrapolation to higher temperatures. Furthermore, preliminary heat capacity measurements of talc between 300° and 700°K (R. A. Robie, personal commun.) are in good agreement (within 2 percent) of that extrapolated from the equation based on low-temperature ($\leq$ 300°K) measurements.

## DISCUSSION

In this section we will use equilibria in the system CaO–MgO–$SiO_2$–$CO_2$–$H_2O$ to examine the consequences of various styles of extra-

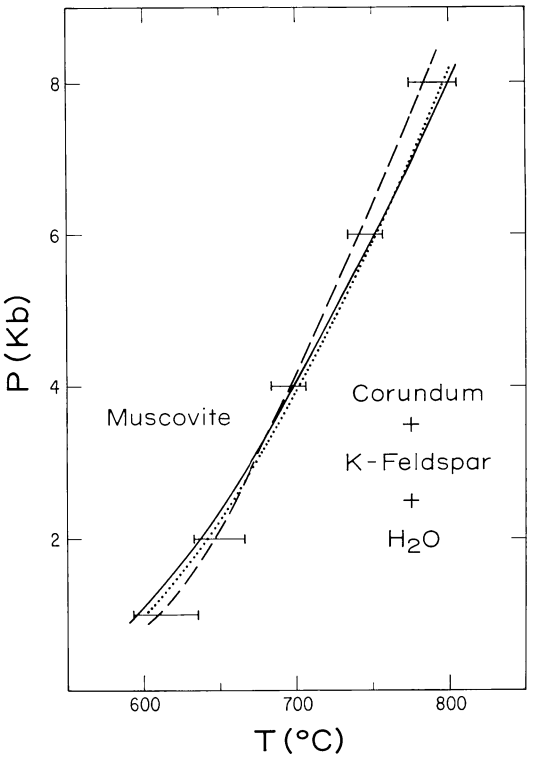


Fig. 12. P–T diagram illustrating various calculated curves for muscovite decomposition as a function of Al–Si order-disorder in muscovite and coexisting K-feldspar. For each of these phases the curves apply either to fully ordered or fully disordered Al/Si distribution. The solid curve is for disordered muscovite and ordered K-feldspar, the dashed curve is for ordered muscovite and disordered K-feldspar, and the dotted curve is for ordered muscovite and ordered K-feldspar. The curve for disordered muscovite and disordered K-feldspar will be identical to that for ordered muscovite and ordered K-feldspar. Experimental brackets are from Chatterjee and Johannes (1974).

polating P–T–X equilibria, followed by some comments on experimentation.

*Isobaric calculations in the system CaO–MgO–$SiO_2$–$CO_2$–$H_2O$.*— Skippen's analysis leads to relatively large errors in the T–X locations of equilibria in the system CaO–MgO–$SiO_2$–$CO_2$–$H_2O$ (fig. 13). To illustrate the importance of data analysis with alternative methods, let us re-examine Skippen's data with a different approach. Returning to figure 6 we note that Skippen obtained one reasonably "tight" experimental bracket (733 ± 7°C) for the talc breakdown reaction using the NB, OH, (X, OH) buffer. Using equation (3) as a base, we have extrapolated the equilibrium curve from this experimental bracket (fig. 6). It is clear that the uncertainties introduced in this type of extrapolation are much smaller than those obtained from Skippen's experimental points (dashed

lines in fig. 6). From our curves, the uncertainty in the A term of the equilibrium constant expression is from −5300 to −5900, arising from the uncertainties in $\Delta S_s$ and $G_{H_2O}$, and producing the hachured error bands in figure 6. The total uncertainty range of the B term of the equilibrium constant, obtained by extrapolating the limits of our error band in figure 6 to the abscissa where $1/T = 0$, is from 9.07 to 9.10. Corresponding uncertainties for the limiting lines fitting Skippen's data (that is, the dashed lines in fig. 6) are −5729 to −11428 for the A term and 8.777 to 14.586 for the B constant. Therefore, our style of calculation results in a smaller error in the equilibrium constant for the reaction compared to the method of Skippen (1974). We calculate the isobaric T–X locations of stable equilibria in the system $CaO–MgO–SiO_2–CO_2–H_2O$ as follows. The narrowest experimental equilibrium brackets of Skippen's (1971) five basic reactions were extrapolated on a T–X section at 2 kb using equation (19). The extremes of each bracket give an upper and lower limit for each extrapolated curve, as shown by the dashed lines in figure 7B. Through coupling the five basic reactions we then calculated the equilibrium temperatures (at $P_f$=2kb and $X_{CO_2}$=0.5) of various equilibria within this system. As an example of this calculation, let us locate Skippen's (1974) reaction:

$$\text{tremolite} + 3\ \text{calcite} + 2\ \text{quartz} = 5\ \text{diopside} + 3\ CO_2 + H_2O \qquad [8]$$

This equilibrium can be derived by coupling his basic reactions:

$$3\ \text{enstatite} + \text{quartz} + H_2O = \text{talc} \qquad [1]$$

$$\text{talc} + 3\ \text{calcite} + 2\ \text{quartz} = 3\ \text{diopside} + 3\ CO_2 + H_2O \qquad [2]$$

$$\text{tremolite} = 2\ \text{diopside} + 3\ \text{enstatite} + \text{quartz} + H_2O \qquad [3]$$

Equation (19) enables calculation of the free energy changes of reactions [1], [2], and [3] at a specified temperature, then permitting calculation of the free energy change of reaction [8], since:

$$(\Delta G_{r\,[8]})_{P,T,X_{CO_2}} = [\Delta G_{r\,[1]} + \Delta G_{r\,[2]} + \Delta G_{r\,[3]}]_{P,T,X_{CO_2}}$$

Such calculations at a variety of temperatures allow determination of the equilibrium where $\Delta G_{r[8]} = 0$. The upper and lower temperature uncertainties for reactions [1], [2], and [3] permit calculation of the corresponding maximum and minimum temperatures for reaction [8] at $X_{CO_2} = 0.5$, which are in turn used as starting points for T–X extrapolation using equation (19). This type of calculation is identical to that of Slaughter, Kerrick, and Wall (1975). Results of this type of calculation are compared with Skippen's method of calculation in figure 13. For many equilibria on this diagram, our calculated uncertainty bands (solid lines) are narrower (and thus more precise) than those of Skippen (dashed lines). In this diagram are included experimental equilibrium brackets obtained in our laboratory, providing an *independent* check on the

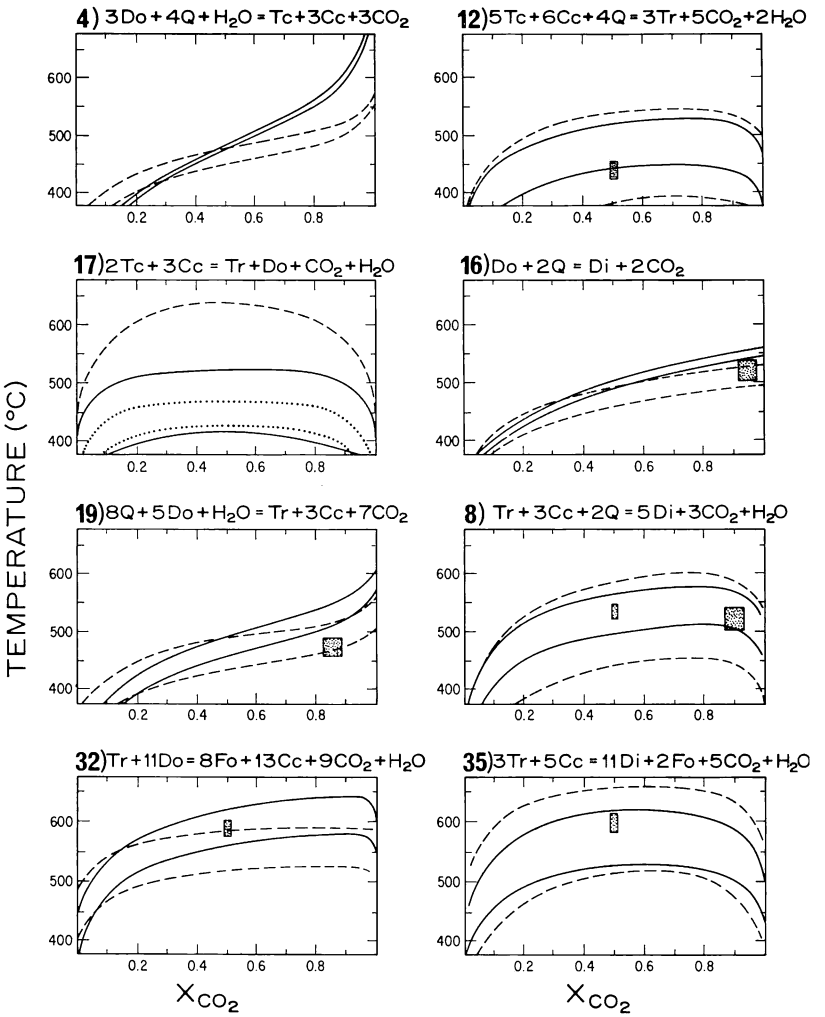


Fig. 13. T–$X_{CO_2}$ diagrams at $P_f = 2$ kb showing total error limits in the location of various equilibria. Dashed lines are limits from Skippen (1974, fig. 5), whereas the solid lines were calculated in this study (see text). Numbers correspond to the equilibria of Skippen (1971, 1974). Stippled areas represent experimental brackets from the following sources: reactions [8], [12], [16], and [19]: Slaughter, Kerrick, and Wall (1975); reactions [32] and [35]: Kerrick and Casquet (in preparation). Dotted curves for reaction [17] are the extremes in location of this equilibrium calculated from the total uncertainty in the location of invariant point B of Slaughter, Kerrick, and Wall (1975, fig. 13).

accuracy of the calculated curves. For reactions [8], [12], [17], [32], and [35], our calculated curves are in agreement with the experimental brackets. Most of the uncertainty shown by Skippen for reactions [8], [12], [17], and [35] is a direct consequence of the large uncertainty introduced in the A and B constants resulting from the reaction:

$$\text{talc} = \text{enstatite} + \text{quartz} + H_2O,$$

as discussed previously. However, for reactions [16] and [19], Skippen's uncertainty bands are in somewhat better agreement with the experimental data than are the curves calculated with our method. The equilibrium constants for reactions [16] and [19] were derived from coupling with that of reaction [4], one of Skippen's five "key" reactions. His equilibrium constant for reaction [4] was based on Gordon and Greenwood's (1970) precise experimental brackets, as shown in figure 2, whereas our curve was extrapolated from Skippen's experimental bracket at $X_{CO_2} \cong 0.2$, assuming ideal mixing. As shown in figure 9, correction for non-ideal mixing would bring our extrapolated curve into good agreement with Gordon and Greenwood's (1970) data, thus yielding agreement with Skippen's dashed curves for reaction [4] in figure 13. Such adjustment in reaction [4] would also bring our calculated curves for reactions [16] and [19] into good agreement with the experimental equilibrium brackets.

Thus, the examples shown in figure 13 illustrate both a major advantage and a major disadvantage of equations derived from log K-1/T plots of experimental data. Where precise control is available for a mixed-volatile equilibrium, as for reaction [4], equations from log K-1/T diagrams insure thermodynamic self-consistency when used to construct T–X diagrams. However, as illustrated by reactions [8], [12], [17], and [35], imprecise experimental control can lead to large uncertainties in the T–X location of equilibria using equations derived from log K-1/T plots of experimental data.

*Polybaric calculations in the system $CaO$–$MgO$–$SiO_2$–$CO_2$–$H_2O$.*— Assuming ideal mixing in the fluid, we can derive the pressure effect of an equilibrium curve for a $H_2O$–$CO_2$ reaction at fixed $X_{CO_2}$ from equation (16):

$$d\Delta G_r = 0 = \Delta V^\circ_r \, dP - \Delta S^\circ_r \, dT + R \, ln \, [X_{CO_2}^{n_{CO_2}} \cdot X_{H_2O}^{n_{H_2O}}] \, dT$$

Rearranging:

$$0 = \Delta V^\circ_r \, dP - (\Delta S^\circ_r + R \, ln \, [X_{CO_2}^{n_{CO_2}} \cdot X_{H_2O}^{n_{H_2O}}]) \, dT$$
$$= \Delta V^\circ_r \, dP - \Delta S_r^{id} \, dT$$

Rearranging yields the Clapeyron equation:

$$\left(\frac{dP}{dT}\right)_{X_{CO_2}} = \frac{\Delta S_r^{id}}{\Delta V^\circ_r} = \frac{\Delta H^\circ_r}{T \, \Delta V^\circ_r}$$

For non-ideal mixtures, the reaction enthalpy would be expressed as:

$$\Delta H^\circ_r = T\Delta S^\circ_r - RT \; ln \; [a_{CO_2}^{n_{CO_2}} \cdot a_{H_2O}^{n_{H_2O}}]$$

Since:

$$\Delta S_r = \Delta S^\circ_r - R \; ln \; [a_{CO_2}^{n_{CO_2}} \cdot a_{H_2O}^{n_{H_2O}}],$$

then:

$$\Delta H^\circ_r = T\Delta S_r$$

Since there appears to be relatively little error introduced by taking $\Delta V^\circ_r$ from tabulated data, the primary uncertainty in P–T slopes stems from errors in $\Delta H^\circ_r$ (or $\Delta S^\circ_r$). The relatively large errors in Skippen's determination of $\Delta H^\circ_r$ and $\Delta S^\circ_r$ lead to correspondingly large errors in the polybaric extrapolation of his equilibria. The importance of this error can be illustrated with the pressure effect on the T–X stability field of the assemblage: talc + calcite. Skippen (1974) *suggests* that the T–X stability field of this assemblage increases with increasing pressure (see figure 14B), although he has clearly indicated the experimental uncertainties in this conclusion. As shown in figure 14D, expansion of the talc + calcite field with increasing pressure implies progressive *divergence* of the temperatures between all stable and metastable equilibria intersecting at the invariant point, whereas diminution of the talc + calcite field implies *convergence* of these equilibria with increasing pressure. Therefore, convergence or divergence can be proven if any two of these equilibria, with their associated uncertainty bands, converge or diverge with increasing pressure. Figure 14E shows a P–T projection at fixed $X_{CO_2}$ of the upper and lower limits of these equilibria as calculated from the equations of Skippen (1974, table 2). It is clear that no two equilibria demonstrate convergence or divergence, such that Skippen's data are inconclusive as to the pressure effect on the talc + calcite stability field. The same conclusion applies to polybaric extrapolations of this type for other values of $X_{CO_2}$.

We now examine the pressure effect on the talc + calcite field through equation (18). Slaughter, Kerrick, and Wall (1975) give the uncertainty limits on the T–X stability field of this assemblage at 2 kb. Taking their lower and upper temperature limits for each of the talc equilibria at $X_{CO_2} = 0.3$, equation (18) was used to extrapolate these equilibria to lower and higher pressures (fig. 14F). It is seen that the talc + calcite stability field diminishes with increasing pressure. It should be emphasized that any adjustments in the upper and lower temperature limits of the talc + calcite field at 2 kb would not affect the conclusion as to the diminution of this field with increasing pressure. These deductions are *independent* of field evidence. Skippen (1974) used natural parageneses as a major argument for expansion of the talc + calcite stability field with increasing pressure. We strongly advocate the integration of data from natural assemblages with experimentally-based

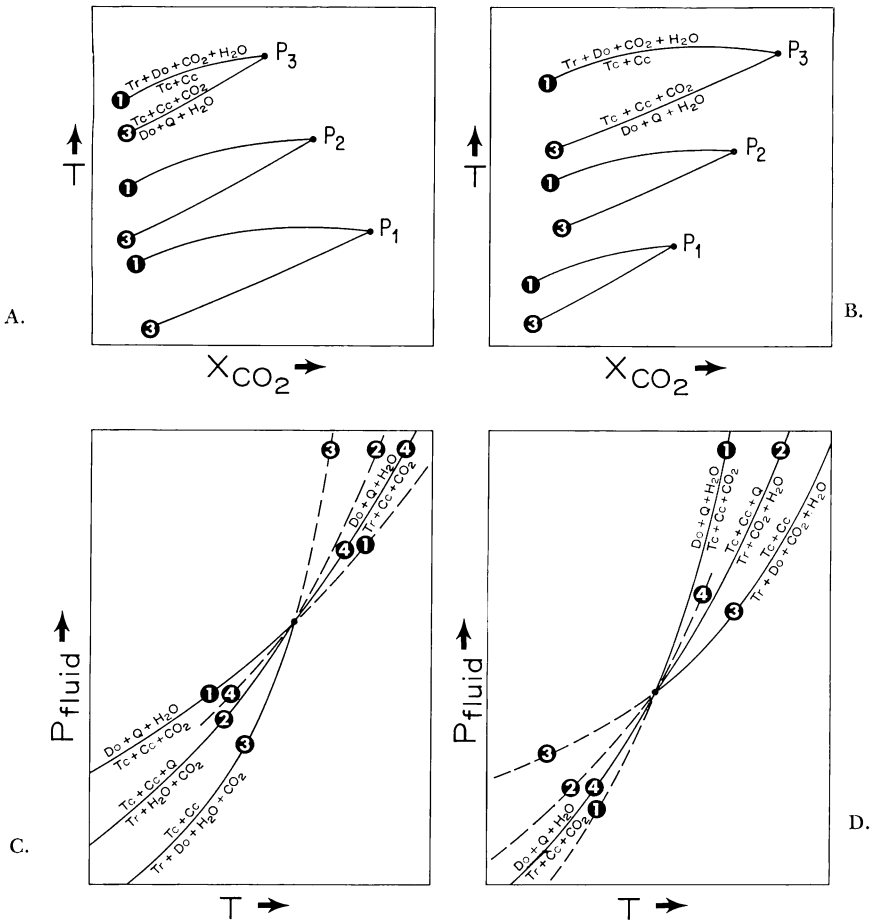


Fig. 14. (A) Schematic T–X diagram showing diminution in the talc + calcite stability field with increasing pressure. $P_1 < P_2 < P_3$. (B) Schematic T–X diagram showing expansion of the talc + calcite stability field with increasing pressure. $P_1 < P_2 < P_3$. (C) Schematic P–T diagram showing key equilibria at fixed $X_{CO_2}$ illustrating the diminution of the talc + calcite stability field with increasing pressures. (D) Schematic P–T diagram showing key equilibria at fixed $X_{CO_2}$ illustrating expansion of the talc + calcite stability field with increasing pressure.

P–T–$X_{CO_2}$ topologies (for example, Kerrick, 1974, p. 757); however, because of the controversy concerning the abundance of talc + calcite in low-pressure versus high-pressure parageneses (Skippen, 1974; Slaughter, Kerrick, and Wall, 1975; Moore and Kerrick, 1976), we are not yet in the position to use field evidence as a check on the pressure effect on the talc + calcite stability field.

*Some guidelines for experimentation.*—For accurate extrapolation of an equilibrium in P–T–$X_{CO_2}$ space, experimental determination of at

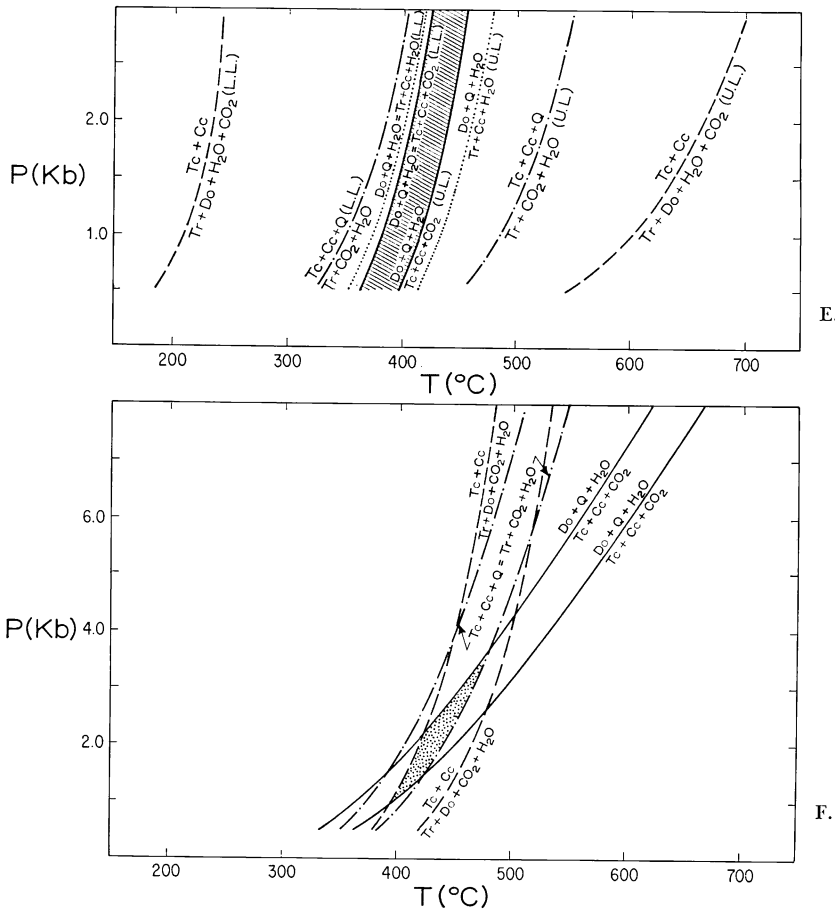


(E) P–T projection at $X_{CO_2} = 0.3$ showing key equilibria relevant to the stability of talc + calcite, calculated from the equations of Skippen (1974). There are two curves for each reaction, one representing the lower temperature limit (L.L.), and the other is the upper temperature limit (U.L.). The hachured area represents mutual overlap of all four equilibria. (F) P–T projection at $X_{CO_2} = 0.3$ showing equilibria extrapolated with equation (18), (see text). Error bands were extrapolated from the limiting 2 kb data of Slaughter, Kerrick, and Wall (1975). Note the correspondence with the schematic P–T diagram (C).

least one narrow (± 5°-10°C) equilibrium bracket is far more useful than several wider equilibrium brackets for the same reaction. However, as illustrated in figure 15, there can be undesirable consequences of extrapolating from an experimental bracket in the extremal ranges of $X_{CO_2}$. Because of the logarithmic dependence of the partial molar free energy of a gas species on its activity ($\overline{G}_i = G°_i + RT\ln a_i$) the partial molar free energy of a gas species (i) will be extremely sensitive to small changes in $X_i$ as $X_i \rightarrow 0$. Thus, for reactions involving a gas species (i), extrapola-

tion from the limiting $X_{CO_2}$ values of a relatively narrow experimental bracket where $X_i \rightarrow 0$ will lead to large differences in the locations of the extrapolated curves. As a practical example, figure 15E shows the reaction:

$$\text{zoisite} + CO_2 = \text{anorthite} + \text{calcite} + H_2O,$$

which has been extrapolated from the extremes of $X_{CO_2}$ within the experimental equilibrium bracket of Storre and Nitsch (1972). The divergence of the extrapolated curves toward lower temperatures, a consequence of the large differences in the partial molar free energies of $CO_2$ at the extremes of the experimental bracket, is analogous to that illustrated in the schematic example in figure 15D. This problem would be avoided by obtaining experimental brackets in the intermediate range of fluid composition ($X_{CO_2} = 0.2 - 0.8$).

For sealed-capsule techniques we have several reasons for preferring experimental determinations of equilibria at $X_{CO_2} = 0.5$. *First,* experi-

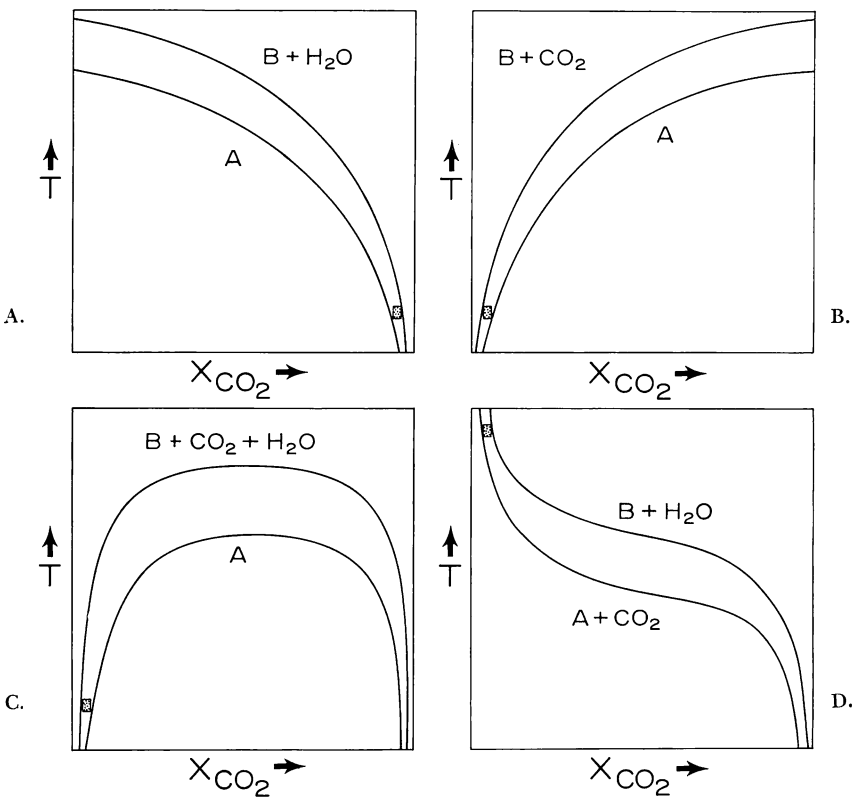


Fig. 15. (A) to (D) Schematic isobaric T–$X_{CO_2}$ diagrams showing errors introduced by extrapolating various types of mixed-volatile equilibria from the end points of equilibrium brackets (stippled). A and B refer to phases or an assemblage of phases.

mental brackets at this fluid composition avoid the large errors in extrapolating from the extremal ranges in $X_{CO_2}$, as illustrated in figure 15. *Secondly,* this fluid composition avoids problems with reaction kinetics at high $X_{CO_2}$ (Slaughter, Kerrick, and Wall, 1975). *Thirdly,* fluids of $X_{CO_2} = 0.5$ can be readily generated by oxalic acid dihydrate, a solid phase at 25°C and 1 atm; hence, the experimental procedure for obtaining this fluid composition is simpler than that for other values of $X_{CO_2}$ (see Kerrick, 1974). *Fourth,* since oxalic acid dihydrate produces a fixed, known $X_{CO_2}$, reaction direction can be monitored by changes in $X_{CO_2}$ from the starting value of $X_{CO_2} = 0.5 \pm 0.01$ (Kerrick, Hunt, and Wall, 1973). However, the positive correlation of temperature and reaction kinetics must also be considered in initially evaluating the experimental conditions for seeking equilibrium. Thus, for the zoisite breakdown reaction at 2 kb, reaction rate will undoubtedly be considerably slower at $X_{CO_2} = 0.5$ than at the higher temperatures investigated by Storre and Nitsch (1972). Furthermore, experimentation in the low-temperature range will be complicated by the $H_2O$–$CO_2$ solvus and consequent profound departure from ideal mixing in the fluid. Therefore, we would again recommend experimental determination at $X_{CO_2} = 0.5$, but at a pressure considerably greater than 2 kb. Since sufficiently accurate P–T–X extrapolations can be carried out with the assumption of ideal mixing (for

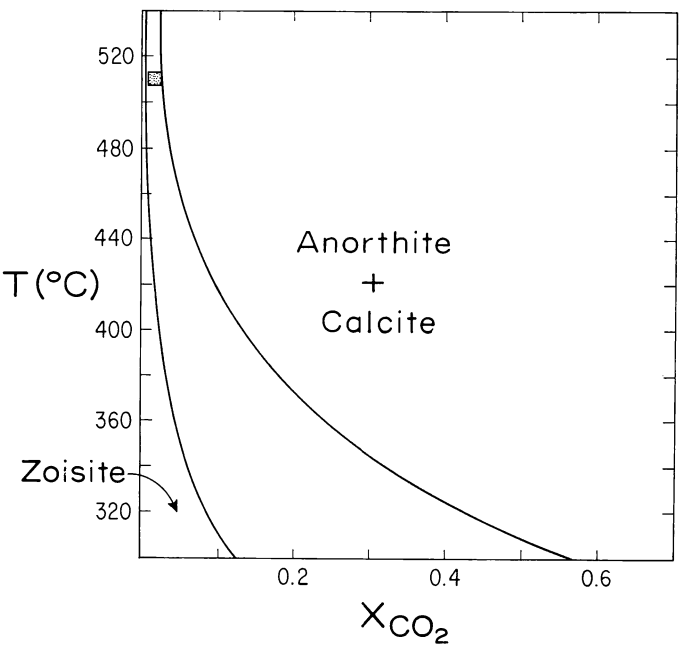


E.

(E) T–$X_{CO_2}$ diagram at $P_f = 2$ kb, showing the reaction: zoisite + $CO_2$ = calcite + anorthite + $H_2O$, extrapolated from the end-points of Storre and Nitsch's (1972) experimental bracket (stippled area).

example fig. 10), the lack of activity data for $H_2O$–$CO_2$ mixtures above 2 kb does not offer a serious drawback to the usefulness of high-pressure experimental brackets for use as starting points for extrapolating equilibria in P–T–X space.

## CONCLUSIONS

Our main objective in this study was to evaluate the various styles of calculating and extrapolating equilibria in P–T–X space. P–T–$X_{CO_2}$ equilibria can be located by: (A) derivation of "coupled equilibria" through appropriate combinations of experimentally-determined stable and/or metastable equilibria, or (B) extrapolation of stable equilibria from experimental equilibrium brackets. Since derivation of stable equilibria by coupling other stable or metastable reactions compounds the uncertainties, we strongly favor the *direct* experimental determination of stable equilibria. With accurate values for the entropies of solid phases and with activity data for $H_2O$–$CO_2$ mixtures, equations (18) and (19) provide accurate P–T–X extrapolation from one or more narrow equilibrium bracket(s). For isobaric extrapolations from an experimental equilibrium bracket, Greenwood's (1967a) equation is quite adequate for routine calculations, providing that a correspondingly accurate $\Delta H^\circ_r$ is available.

Fundamentally, the equilibrium constant approach is capable of providing accurate equations for extrapolating equilibria in P–T–$X_{CO_2}$ space. However, if equations of *low uncertainty* are to be derived from experimental data it is imperative that for each equilibrium there are *at least* two narrow experimental brackets at widely-spaced temperatures. In the case of Skippen's work, large uncertainties in two of his five experimentally-determined equilibria resulted in correspondingly large uncertainties in the equations for equilibria derived by coupling these basic reactions. Where only one narrow experimental bracket is available, as in figure 6, we advocate extrapolation from this bracket using equations (18) and (19) rather than extrapolating from an equation of high uncertainty derived from considering experimental data only (that is from a log K-1/T diagram). Undoubtedly, the largest potential source of error in our method stems from absolute errors in high-temperature entropies of solid phases (tabulated in Robie and Waldbaum, 1968). Aside from the notorious problem of the configurational entropies of aluminous phases, as discussed previously, we are aware of potential errors in the entropies of non-aluminous phases. Thus, we do not advise accepting extrapolations based on tabulated thermochemical data without some independent check. Intercomparison of extrapolations based on thermochemical data with experimental results is a necessary evaluation of the accuracy of thermochemical data (for example, Zen, 1972; Gordon, 1973). For the system CaO–MgO–$SiO_2$–$CO_2$–$H_2O$, P–T–$X_{CO_2}$ extrapolation utilizing expressions involving high-temperature entropies are internally consistent, that is, an equilibrium extrapolated from one narrow experimental bracket passes through other narrow experimental brackets (Slaughter,

Kerrick, and Wall, 1975). This would suggest no significant errors in the high temperature entropies of the solid phases involved in these equilibria.

ACKNOWLEDGMENTS

We are very grateful to G. M. Anderson, T. M. Gordon, and D. A. Hewitt, for critically reviewing an early draft of this paper. This research was supported by grant GA-25685 from the Earth Sciences Section of the National Science Foundation.

REFERENCES

Althaus, Egon, Karotke, E., Nitsch, K. H., and Winkler, H. G. F., 1970, An experimental re-examination of the upper stability limit of muscovite plus quartz: Neues Jahrb. Mineralogie Monatsh., v. 7, p. 325-336.

Anderson, G. M., 1970, Some thermodynamics of dehydration equilibria: Am. Jour. Sci., v. 269, p. 392-401.

Birch, F., 1966, Compressibility; elastic constants, *in* Clark, S. P., Jr., ed., Handbook of Physical Constants: Geol. Soc. America Mem. 97, p. 97-173.

Burnham, C. Wayne, Holloway, J. R., and Davis, N. F., 1969, Thermodynamic properties of water to 1000°C and 10,000 bars: Geol. Soc. America Spec. Paper 132, 96 p.

Cameron, M., Sueno, S., Prewitt, C. T., and Papike, J. J., 1973, High-temperature crystal chemistry of acmite, diopside, hedenbergite, jadeite, spodumene, ureyite: Am. Mineralogist, v. 58, p. 649-664.

Chatterjee, N. D., 1970, Synthesis and upper stability of paragonite: Contr. Mineralogy Petrology, v. 27, p. 244-257.

Chatterjee, N. D., and Johannes, W., 1974, Thermal stability and standard thermodynamic properties of synthetic $2M_1$–Muscovite, $K\ Al_2[Al\ Si_3O_{10}(OH)_2]$: Contr. Mineralogy Petrology, v. 48, p. 89-114.

Chernosky, J. V., Jr., 1974, The upper stability of clinochlore at low pressure and the free energy of formation of Mg–cordierite: Am. Mineralogist, v. 59, p. 496-507.

Franck, E. V., and Tödheide, K., 1959, Thermische eigenschaften überkritischer Mischungen von kohlendioxyd und wasser bis zu 750°C und 2000 atm: Zeitschr. für Phys. Chemie, v. 22, p. 232-245.

Goldsmith, J. R., and Heard, H. C., 1961, Subsolidus phase relations in the system $CaCO_3$–$MgCO_3$: Jour. Geology, v. 69, p. 45-74.

Gordon, T. M., 1973, Determination of internally consistent thermodynamic data from phase equilibrium experiments: Jour. Geology, v. 81, p. 199-208.

Gordon, T. M., and Greenwood, H. J., 1970, The reaction: dolomite + quartz + water = talc + calcite + carbon dioxide: Am. Jour. Sci., v. 268, p. 225-242.

Greenwood, H. J., 1967a, Mineral equilibria in the system $MgO$–$SiO_2$–$H_2O$–$CO_2$, *in* Abelson, P. H., ed., Researches in Geochemistry, v. 2: New York, John Wiley & Sons, p. 542-567.

———— 1967b, Wollastonite: stability in $H_2O$–$CO_2$ mixtures and occurrence in a contact-metamorphic aureole near Salmo, British Columbia, Canada: Am. Mineralogist, v. 52, p. 1669-1680.

Hewitt, D. A., 1973, Stability of the assemblage muscovite–calcite–quartz: Am. Mineralogist, v. 58, p. 785-791.

Kelley, K. K., 1960, Contributions to the data of theoretical metallurgy XIII. High temperature heat-capacity, and entropy data for the elements and inorganic compounds: U.S. Bur. Mines Bull. 584, 232 p.

Kerrick, D. M., 1972, Experimental determination of muscovite + quartz stability with $P_{H_2O} < P_{total}$: Am. Jour. Sci., v. 272, p. 946-958.

———— 1974, Review of metamorphic mixed-volatile equilibria: Am. Mineralogist, v. 59, p. 729-762.

Kerrick, D. M., and Darken, L. S., 1975, Statistical thermodynamic models for ideal oxide and silicate solid solutions, and application to plagioclase: Geochim. et Cosmochim. Acta., v. 39, p. 1431-1442.

Kerrick, D. M., Hunt, J. A., and Wall, V. J., 1973, Experiments on some equilibria involving calc–silicate phases: Geol. Soc. America Abs. with Program, v. 5, p. 693.

Moore, J. N., and Kerrick, D. M., 1976, Equilibria in siliceous dolomites of the Alta aureole, Utah: Am. Jour. Sci., v. 276, p. 502-524.

Robie, R. A., Bethke, P. M., and Beardsley, K. M., 1967, Selected X-ray crystallographic data, molar volumes, and densities of minerals and related substances: U.S. Geol. Survey Bull. 1248, 87 p.

Robie, R. A., and Stout, J. W., 1963, Heat capacity from 12 to 305°K, and entropy of talc and tremolite: Jour. Phys. Chemistry, v. 67, p. 2252-2256.

Robie, R. A., and Waldbaum, D. R., 1968, Thermodynamic properties of minerals and related substances at 298.15°K (25°C) and one atmosphere (1.013 bars) pressure and at higher temperatures: U.S. Geol. Survey Bull. 1259, 256 p.

Ryzhenko, B. N., and Malinin, S. D., 1971, The fugacity rule for the systems $CO_2$–$H_2O$–$CO_2$–$CH_4$, $CO_2$–$N_2$, and $CO_2$–$H_2$: Geochemistry Internat., p. 562-574.

Skinner, B. J., 1966, Thermal expansion, *in* Clark, S. P., Jr., ed., Handbook of Physical Constants: Geol. Soc. America Mem. 97, p. 75-96.

Skippen, G. B., 1971, Experimental data for the reactions in siliceous marbles: Jour. Geology, v. 79, p. 457-481.

———— 1974, An experimental model for low pressure metamorphism of siliceous dolomitic marble: Am. Jour. Sci., v. 274, p. 487-509.

Skippen, G. B., and Hutcheon, I., 1974, The experimental calibration of continuous reactions in siliceous carbonate rocks: Canadian Mineralogist, v. 12, p. 327-333.

Slaughter, J., Kerrick, D. M., and Wall, V. J., 1975, Experimental and thermodynamic study of equilibria in the system CaO–MgO–$SiO_2$–$H_2O$–$CO_2$: Am. Jour. Sci., v. 275, p. 143-162.

Slaughter, J., Wall, V. J., and Kerrick, D. M., 1976, APL computer programs for thermodynamic calculations of equilibria in P–T–$X_{CO_2}$ space: Contr. Mineralogy Petrology, v. 54, p. 157-171.

Smith, J. V., 1974, Feldspar Minerals. V. 1: Crystal Structure and Physical Properties: New York, Springer Verlag, 627 p.

Storre, B., and Nitsch, K. H., 1972, Die reaktion 2 Zoisite + 1 $CO_2$ = 3 Anorthite + 1 Calcite + 1 $CO_2$: Contr. Mineralogy Petrology, v. 35, p. 1-10.

Stout, J. W., and Robie, R. A., 1963, Heat capacity from 11 to 300°K, entropy, and heat of formation of dolomite: Jour. Phys. Chemistry, v. 67, p. 2248-2252.

Stull, D. R., and Prophet, H., 1971, JANAF Thermochemical tables, 2 ed.: Midland Mich., Dow Chemical Co.

Sueno, S., Cameron, M., Papike, J. J. and Prewitt, C. T., 1973, The high temperature crystal chemistry of tremolite: Am. Mineralogist, v. 58, p. 649-664.

Taylor, L. A., and Bell, P. M., 1971, Thermal expansion of pyrophyllite: Carnegie Inst. Washington Year Book 69, p. 193-194.

Wall, V. J., and Essene, E., 1972, Subsolidus equilibria in CaO–$Al_2O_3$–$SiO_2$–$H_2O$: Geol. Soc. America Abs. with Program, v. 4, p. 700.

Zen, E-an, 1972, Gibbs free-energy, enthalpy, and entropy of ten rock-forming minerals; calculations, discrepancies, and implications: Am. Mineralogist, v. 57, p. 524-553.